Diverging future surface mass balance between the Antarctic ice shelves and grounded ice sheet

Christoph Kittel [1], Charles Amory [1,2], Cécile Agosta [3], Nicolas C. Jourdain [2], Stefan Hofer [4], Alison Delhasse [1], Sébastien Doutreloup [1], Pierre-Vincent Huot [5], Charlotte Lang [1], Thierry Fichefet [5], and Xavier Fettweis [1]

[1]Department of Geography, UR SPHERES, University of Liège, Belgium
[3]Laboratoire des Sciences du Climat et de l'Environnement, LSCE-IPSL, CEA-CNRS-UVSQ, Université Paris-Saclay, Gif-sur-Yvette, France
[2]Univ. Grenoble Alpes/CNRS/IRD/G-INP, IGE, Grenoble, France
[4]Department of Geosciences, University of Oslo, Oslo, Norway
[5]Earth & Climate, Earth and Life Institute, Catholic University of Louvain, Louvain-la-Neuve, Belgium

Correspondence: Christoph Kittel (ckittel@uliege.be)

Abstract. The future surface mass balance (SMB) will influence the ice dynamics and the contribution of the Antarctic ice sheet (AIS) to the sea-level rise. Most of recent Antarctic SMB projections were based on the 5th phase of the Coupled Model Intercomparison Project (CMIP5). However, new CMIP6 results have revealed a $+1.3°C$ higher mean Antarctic near-surface temperature than in CMIP5 at the end of the 21st century enabling estimations of future SMB in warmer climates. Here, we investigate the AIS sensitivity to different warmings with an ensemble of four simulations performed with the polar regional climate model MAR forced by two CMIP5 and two CMIP6 models over 1981–2100. Statistical extrapolation allows us to expand our results to the whole CMIP5 and CMIP6 ensembles. Our results highlight a contrasting effect on the future grounded ice sheet and the ice shelves. The SMB over grounded ice is projected to increase as a response to stronger snowfall, only partly offset by enhanced meltwater runoff. This leads to a cumulated sea-level rise mitigation (i.e. an increase in surface mass) of the grounded Antarctic surface by 5.1 ± 1.9 cm sea-level equivalent (SLE) in CMIP5-RCP8.5 and 6.3 ± 2.0 cm SLE in CMIP6-ssp585. Additionally, the CMIP6 low-emission ssp126 and intermediate-emission ssp245 scenarios project a stabilised surface mass gain resulting in a lower mitigation to sea-level rise than in ssp585. Over the ice shelves, the strong runoff increase associated with higher temperature is projected to decrease the SMB (more strongly in CMIP6-ssp585 compared to CMIP5-RCP8.5). Ice shelves are however predict to have a close-to-present-equilibrium stable SMB under CMIP6 ssp126 and ssp245 scenarios. Future uncertainties are mainly due to the sensitivity to anthropogenic forcing and the timing of the projected warming. While ice shelves should remain at a close-to-equilibrium stable SMB under the Paris Agreements, MAR projects strong SMB decrease for an Antarctic near-surface warming above $+2.5°C$ limiting the warming range before potential irreversible damages on the ice-shelves. Finally, our results reveal the existence of a potential threshold ($+7.5°C$) that leads to a lower grounded SMB increase. This however has to be confirmed in following studies using more extreme or longer future scenarios.

1 Introduction

The surface mass balance (SMB) of the Antarctic ice sheet (AIS) is the resultant of accumulation through snowfall and ablation through surface erosion, sublimation and runoff. Positive (negative) SMB values reflect a mass gain (loss) at the surface of the ice sheet. The AIS currently loses mass mainly by ice discharge and basal melting. The difference between SMB and ice discharge determines the sea-level rise contribution of the AIS. Due to the large amount of grounded ice, the AIS is the largest potential contributor among the cryosphere (58 m sea-level equivalent (SLE), Fretwell et al., 2013; Morlighem et al., 2020). Although not directly contributing to sea-level variations, relatively-flat and large ice shelves, i.e. the floating extensions of the ice sheet, nevertheless influence the ice dynamics by restraining the ice over the grounded continent that flows under the force of gravity toward the ocean. This buttressing effect first limits glacier-flow acceleration and then control ice discharge (e.g., Rignot et al., 2004; Dupont and Alley, 2005; Gudmundsson, 2013; Fürst et al., 2016).

Since the 2000s, the Antarctic ice sheet has been losing mass at an accelerating rate mainly due to an increased ice discharge in the West AIS (Shepherd et al., 2018), itself caused by the acceleration of outlet glaciers in response to basal (ocean) melt thinning the ice shelves and reducing their buttressing effect (Paolo et al., 2015; Gardner et al., 2018; Rignot et al., 2019). Stronger basal melting of ice shelves is further projected to drive future Antarctic mass loss (Holland et al., 2019; Seroussi et al., 2020). Despite stable surface melt rates since 1979 (Kuipers Munneke et al., 2012), atmospheric conditions through intense melt events can lead to meltwater ponding at the surface of ice shelves, increasing their potential for hydrofracturing (Scambos et al., 2000; van den Broeke, 2005). The resulting ice-shelf collapses over the Antarctic Peninsula then caused enhanced ice discharge (Scambos et al., 2004, 2014), highlighting the important role of atmosphere-surface interactions in the AIS stability, likely to become even more important in the context of global warming.

With increasing temperatures, more surface mass gain is expected over the AIS as a result of an increase in precipitation (Palerme et al., 2017; Gorte et al., 2019). Frieler et al. (2015) suggested an increase in accumulation linked to air temperature of $\sim 6\% \, °C^{-1}$ that is confirmed by SMB reconstructions from ice cores over the 20th century (Medley et al., 2018; Medley and Thomas, 2019), but not retrieved in recent (too short) SMB reconstructions (Van Wessem et al., 2018; Agosta et al., 2019; Mottram et al., 2020) due to the internal climate variability determining precipitation pattern (Previdi and Polvani, 2016). For moderate warming, increase in snowfall is likely to outpace increased losses through ablation and especially runoff making the Antarctic SMB the only future mitigating contributor to sea-level rise (Krinner et al., 2007; Agosta et al., 2013; Ligtenberg et al., 2013; Lenaerts et al., 2016; Garbe et al., 2020). Melt increase under the high emissions pathway by 2100 is however projected to be large enough to enhance ice-shelf collapses (Trusel et al., 2015; Donat-Magnin et al., 2020). The future of ice shelves experiencing more snowfall that can enable the snowpack to absorb more liquid water, is still uncertain even if the firn air content should decrease (Ligtenberg et al., 2014; Donat-Magnin et al., 2020), suggesting an increased risk of hydrofracturing and collapse (Kuipers Munneke et al., 2014).

The most recent projections of the Antarctic SMB are based on global climate models and Earth System Models (ESMs) of the 5th phase of the Coupled Model Intercomparison Project (CMIP5) (Taylor et al., 2012), whereas new climate projections are now available through CMIP6 (O'Neill et al., 2016). Under the highest emission scenario, projections for the AIS annual

mean near-surface temperature in 2100 are +1.3°C higher in CMIP6 models than in CMIP5 models (Fig. 1). However, using these climate models outputs directly to study the evolution of the SMB often involves several compromises: (i) their resolution remains too coarse to correctly represent the steep margins of the ice sheet or the peripheral ice shelves (Seroussi et al., 2020) and (ii) they do not account properly for important physical processes of polar regions, in particular those related to the stable boundary layer and snow metamorphism, snowmelt, albedo feedbacks, and refreezing in the snowpack (Lenaerts et al., 2016; Favier et al., 2017). This partly explains why the SMB derived from ESMs has often been roughly approximated as precipitation minus evaporation even for projections (e.g., Palerme et al., 2017; Favier et al., 2017; Gorte et al., 2019; Seroussi et al., 2020) or included a runoff computed from non-polar-oriented models (Golledge et al., 2015; Nowicki et al., 2020; Garbe et al., 2020), although a few exceptions exist (e.g., Lenaerts et al., 2016; Sellar et al., 2019).

Dynamical downscaling of ESMs (hereafter designating both global climate models and new-generation Earth System Models without any consideration of the model sophistication to represent the carbon cycle or cloud-aerosol interactions) with polar-oriented regional climate models (RCMs) offers an alternative to address not only the issue of coarse spatial resolution, but also more importantly to more robustly evaluate changes in mass and energy fluxes at the ice-sheet surface (e.g., Fyke et al., 2018; Lenaerts et al., 2019; Fettweis et al., 2020). This is why we propose here to use the polar-oriented RCM MAR, widely used over the AIS (e.g., Kittel et al., 2018; Agosta et al., 2019; Wille et al., 2019) to downscale an ensemble of 4 different ESMs from the CMIP5 and CMIP6 exercises, selected to cover a wide range of near-surface warming (+3.2°C to +8.5°C over the Antarctic ice sheet during the 21st century and then statistically extrapolate our results to the full CMIP5 and CMIP6 ensembles. This study therefore aims to (1) quantify the surface response of the AIS to warmer climates, and more specifically the different responses of the grounded ice and ice shelves using both new scenarios and an adapted representation of polar processes, (2) discuss the evolution of individual SMB components including future runoff ablation that can significantly compensate for mass gained through snowfall, (3) assess the future contribution (and related uncertainties) of the grounded Antarctic SMB to sea-level rise and the future state of the peripheral ice shelves using all the CMIP5 and new CMIP6 models with different emissions scenarios by extrapolating RCM-derived SMB projections.

2 Methods

2.1 The regional atmospheric model MAR

MAR is a polar-oriented regional climate model frequently used to study the Antarctic (e.g., Amory et al., 2015; Kittel et al., 2018; Agosta et al., 2019) and Greenland (e.g., Fettweis et al., 2017; Hofer et al., 2017; Delhasse et al., 2019) ice sheet climates. MAR is a hydrostatic model relying on the primitive equations described in Gallée and Schayes (1994). The model includes a cloud microphysics module solving conservation equations for five water species: snow particles, cloud ice crystals, rain drops, cloud droplets and specific humidity (Gallée, 1995). Airborne particles can be advected vertically from one atmospheric layer to another and notably contribute through sublimation to the heat and moisture budget of the atmosphere (Agosta et al., 2019). The radiative transfer scheme is adapted from ECMWF ERA-40 reanalysis (Morcrette, 2002). The transfer of mass and energy between the surface and the atmosphere is simulated in the 1-D surface scheme SISVAT (Soil Ice Snow Vegetation
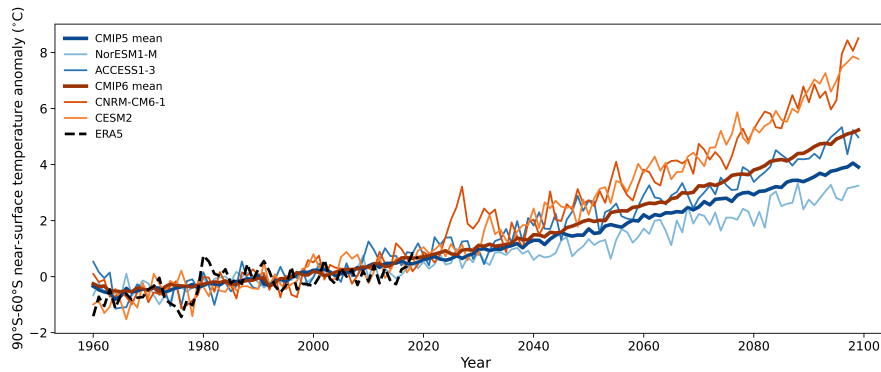
Figure 1. Time series of the 90°S–60°S annual near-surface temperature anomaly (°C) compared to the present reference period (1981–2010) from the ERA5 reanalysis and ESMs using the extreme high-emission scenarios RCP8.5 and ssp585 after their historical period (2004 for CMIP5 and 2014 for CMIP6). The thick blue and red lines represent the mean annual warming from 28 CMIP5 and 34 CMIP6 ESMs. Thinner orange and blue lines are for ESMs selected as boundary conditions for our regional climate model MAR: CNRM-CM6-1 and CESM2 (CMIP6, ssp585) and NorESM1-M and ACCESS1-3 (CMIP5, RCP85). The dashed black line is the ERA5 reanalysis (1960–2020) (Hersbach et al., 2020).

Atmosphere Transfer; De Ridder and Gallée, 1998) module, which consists of soil and vegetation (De Ridder and Schayes, 1997), snow (Gallée and Duynkerke, 1997; Gallée et al., 2001) and ice (Lefebre et al., 2003) sub-modules. The latter two
90   are originally based on the snow model CROCUS (Brun et al., 1992). The dynamical snow and ice components represent snow properties and metamorphism across 30 snow/firn/ice layers resolving the 20 first meters of snow/ice. SISVAT solves the surface energy budget using excess in energy to melt the snow. Each snow/firn layer has a maximum water retention of 5%, while the remaining liquid water - coming from rainfall or surface meltwater - can freely percolate downward as long as the underlying snow density does not reach a close-off density of $830\,\mathrm{kg\,m^{-3}}$. Remaining liquid water beyond the snowpack
95   saturation is converted into surface runoff, meaning that in the absence of water-routing hydrologic scheme, all surface water that could potentially form melt ponds is considered as runoff, i.e., is lost by the ice sheet. Snow/ice surface albedo varies as a function of the optical properties of snow, the presence of bare ice or liquid water, the snow depth over ice and clouds (Tedesco et al., 2016) with a maximum value of 0.94 for fresh snow and a minimum value of 0.55 for bare ice over Antarctica.

   In this study, we used the latest MAR version (3.11), hereafter called MAR. The latest updates in MAR improve the cloud
100   lifetime, the model stability, its computational efficiency and reduce the dependency to the model time-step. Several other improvements have also been made in MAR and relative to the previous model versions used over Antarctica (Agosta et al., 2019) and are detailed below:

   a. Inclusion of rock outcrops in the ice-sheet mask enabling potential feedbacks between low-albedo exposed rocks (0.17 in MAR) and enhanced snow melting (e.g., Kingslake et al., 2017) around pixels partially composed of rocks. This also
105   resulted in the ice mask being enlarged at the margins while reducing the ice sheet area. SISVAT computes the different

exchanges for the rock surface separately from the snow/firn/ice covered part and then weight-aggregates them according to the proportion of each sub-grid cell.

b. Addition of a vertical atmospheric level (from 23 to 24) for a CPU-allocation reason (better parallelisation along the vertical axis). Note that MAR near-surface results are not sensitive to the additions of more atmospheric levels (Amory et al., 2020(in preperation)).

c. Modification of the fresh falling snow density, now computed as a function of the $10\,\mathrm{m}$ wind speed ws_{10} ($\mathrm{m\,s^{-1}}$) only:

$$\rho_s = 200 + 32\,ws_{10}, \tag{1}$$

with minimum and maximum values fixed to 300 and $400\,\mathrm{kg\,m^{-3}}$ in accordance with observations (Agosta et al., 2015, Table S2) and the new developments into the drifting-snow scheme (Amory et al., 2020(in preperation)).

The Antarctic topography, and ice/rock fraction are computed from the 1 km resolution digital elevation model Bedmap2 (Fretwell et al., 2013). The ice mask is fixed and cannot evolve, meaning that changes in ice extent following for instance an ice-shelf collapse are not represented. The same is true for surface elevation that is assumed to remain constant in the absence of ice dynamics and evolving topography. Therefore, feedbacks between the ice sheet geometry and the atmosphere are not taken into account in our simulations. Finally, as the drifting-snow scheme (Amory et al., 2020(in preperation)) was still under development when we performed our simulations, it was not activated in this study.

2.1.1 Selection of ESMs

Large-scale forcing models were chosen among the CMIP5 and CMIP6 ESMs. CMIP6 models rely on an improved and more sophisticated representation of the global climate system than CMIP5. They incorporate better coupling between the different components of the Earth system, improved present- and better-constrained future concentrations scenarios of long-lived greenhouse gases and aerosols (Eyring et al., 2016; O'Neill et al., 2016). Additionally, most CMIP6 ESMs are also run at a higher spatial resolution. First analyses of the CMIP6 results revealed higher equilibrium climate sensitivity in this new-generation models (Mauritsen et al., 2019; Voldoire et al., 2019; Zelinka et al., 2020; Meehl et al., 2020; Wyser et al., 2020), suggesting warmer future climates, while based on similar future scenarios in terms of global radiative forcing. However, this higher climate sensitivity is potentially not supported by paleo-climate records (Zhu et al., 2020). We therefore also included models from the CMIP5 dataset, some of which show a good comparison with reanalyses over the current Antarctic climate (Agosta et al., 2015; Palerme et al., 2017). We only chose the scenarios of the largest greenhouse gas emissions from CMIP5 (RCP8.5) and its updated version in CMIP6 (ssp585) in order to obtain stronger warming signals and then SMB sensitivities. These two scenarios have an equivalent global radiative forcing of $+8.5\,\mathrm{W\,m^{-2}}$ by 2100, but differ in how the anthropogenic forcing is split between individual drivers of global warming (O'Neill et al., 2016).

The selection of ESMs that were dynamically downscaled by MAR was based on their ability to i) represent the current climate (air temperature and humidity, sea surface conditions, and large-scale circulation) around the AIS and ii) diversify the projected changes during the 21st century. These criteria ensure on one hand, that the ESM biases will not have a prejudicial

effect on the projections since the present state determines future biases (Agosta et al., 2015; Krinner and Flanner, 2018) and on the other hand that we assess the AIS response to a wide range of projected temperature increases for a better quantification of the future uncertainties for a same scenario. We therefore firstly ranked ESMs by comparing them to the ECMWF reanalysis ERA5 (Hersbach et al., 2020) over the recent "historical" period (1980–2004) following the method defined in Agosta et al. (2015) and Barthel et al. (2020) for CMIP5, extended here to CMIP6 and applied only to the Antarctic atmosphere. The method firstly computes the root mean square error (RMSE) compared to ERA5 for several climate variables (mean air temperature at 850 hPa, annual precipitable water, annual sea level pressure, summer sea surface temperature and winter sea ice extent over 1980–2004) that are supposed to determine the SMB (Agosta et al., 2015). The score of each ESM is then obtained by averaging its RMSEs that were previously normalized with regards to the multi-model median and interquartile range. This enables the combination of several metrics using the same weight for each of the metrics. Once the models were ranked on the basis of their score against ERA5, the final selection was made to diversify the changes expected at the end of the century and the availability of 6-hourly outputs in the CMIP5/CMIP6 database at the end of 2019 when we started our experiments.

We selected two models from the CMIP5 ensemble, ACCESS1.3 and NorESM-M, and two from CMIP6, CNRM-CM6-1 and CESM2. The Antarctic (90°S–60°S) near-surface warming they produce for RCP8.5 (CMIP5) and ssp585 (CMIP6) is shown in Fig. 1. Figure. 1 also illustrates that ESMs correctly reproduce the mean warming since 1960. ACCESS1.3 (Bi et al., 2013; Dix et al., 2013) is the model that best represents the present Antarctic climate compared to ERA-Interim (Agosta et al., 2015), and is also among the best models when compared to ERA5 (Agosta et al., in preparation). This ESM has a near-surface Antarctic warming close to the CMIP6 multi-model mean (+5°C,). NorESM1-M (Bentsen et al., 2013; Iversen et al., 2013) projects a weaker Antarctic atmospheric warming (+3.2°C, Fig. 1) but a stronger ocean warming (Barthel et al., 2020). CNRM-CM6-1 (Voldoire et al., 2019) correctly represents the present Antarctic climate and was among the first models available in the CMIP6 data base. This model also enables to assess the AIS response to an extreme Antarctic warming (+8.5°C) since it is the warmest model over the AIS among the CMIP5 and CMIP6 databases at the end of the 21st century. CESM2 (Danabasoglu et al., 2020) has a lower score than half of the CMIP5 and CMIP6 models compared to ERA5 (Agosta et al., in preparation). Despite its modest ranking, it was chosen due to its relatively detailed representation of polar oriented processes, early availability, and the frequent use of this model and its earlier version to study the AIS (e.g., Lenaerts et al., 2016; Fyke et al., 2017; Medley et al., 2018; Nowicki et al., 2020). Its projected warming (+7.7°C) is close to the mean warming projected by CNRM-CM6-1. From this perspective, selecting both CESM2 and CNRM-CM6-1 does not maximise the warming range covered and prevents our selected ESM ensemble to be representative of the mean CMIP5 and CMIP6 warming. Yet, it enables us to assess the AIS response (and uncertainties) related to the strong warming that is only projected by a few ESMs.

2.1.2 Experiments

MAR is forced by 6-hourly large-scale forcing fields at its atmospheric lateral boundaries (pressure, wind, specific humidity, and temperature), at its sea surface (sea ice concentration and sea surface temperature), as well as at the top of the troposphere (wind and temperature). We forced MAR with the selected ESMs over 1976–2100 (Sect. 2.1.1), and the first five years (1976–1980) were discarded as spinup. The simulations are called MAR(ACCESS1.3), MAR(CESM2), MAR(CNRM-CM6-1), and

MAR(NorESM1-M) hereafter. We used the same intermediate spatial resolution (35 km) as in (Agosta et al., 2019) and (Mottram et al., 2020) as a computation time compromise to run the model with multiple forcings over the 20th and the 21st centuries. In order to assess the quality of the downscaling over the present climate, we also forced MARv3.11 by the ERA5 reanalysis (MAR(ERA5) hereafter). This comparison between MAR forced by the different ESMs, as well as an evaluation of MAR(ERA5), is available as supplementary material. It shows that MAR(ERA5) performs similarly as MARv3.10 forced by ERA-Interim, which was among the best simulations in terms of both present Antarctic near-surface climate and SMB in the recent evaluation conducted by Mottram et al. (2020). We refer to Supplement S1 for more details about the comparison and evaluation of MARv3.11 in terms of near-surface climate, melt and SMB.

In this study, we have chosen to define the reference period of the present climate as 1981–2010. This 30-year reference period coincides with the availability of reanalyses and is a compromise between the end of the historical scenarios, which last until 2004 for CMIP5 and 2014 for CMIP6. Furthermore, Mottram et al. (2020) showed that this period is characterised by a relatively stable SMB over Antarctica. Projected SMB and components values are given compared to their respective mean values over current climate to remove the dependence of the potential linear biases over current climate but raw values over the grounded ice sheet and ice shelves are available in Supplement (Tab. S3).

3   Evaluation of MAR(ESM) simulations over present

Present biases might have a significant influence on the projections results and remain in the future (Fettweis et al., 2013; Agosta et al., 2015; Krinner and Flanner, 2018; Fettweis et al., 2020), highlighting the need for a thorough evaluation over the present climate. Since ESMs only simulate meteorological conditions representative of a certain climate, evaluating MAR ESM-forced simulations cannot be done using the observations directly. We then compared these simulations to the averaged MAR(ERA5) hereafter considered as a reference and evaluated in Sect. S1.

MAR(ACCESS1.3) is the experiment that best compares with the reference MAR(ERA5) over the present climate. It displays the lowest integrated-SMB anomaly (Tab. S2) and spatial RMSE and bias (Fig. 2). MAR(ACCESS1.3) underestimates SMB over Wilkes Land, Queen Mary Land and the Amundsen sector while it overestimates SMB over Queen Maud Land and the lee side of the Antarctic Peninsula. These negative anomalies are associated with the small underestimation of the summer and winter precipitable water in ACCESS1.3 (Agosta et al., 2015).This experiment also reveals mostly non-significant temperature biases in summer (Fig. S3), except for a small negative bias over Ross and Rhone ice shelves, yielding very similar integrated melt values.

MAR(NorESM1-M) presents mostly non-significant anomalies compared to MAR(ERA5) but overestimates the mean integrated annual SMB as a consequence of an overestimation of the snowfall and to, a lesser extent, a lower surface ablation (Tab. S2). Higher snowfall values are modelled over Marie Byrd Land, the Peninsula, and the Brunt ice shelf whiler lower values compensate this overestimation over Queen Mary Land, Wilkes Land and the Amery ice shelf (Fig. S4), which are strongly linked with the humidity anomalies in the forcing ESM(Agosta et al., 2015). NorESM1-M being too cold (with lower free atmosphere summer and ocean temperatures as well as higher sea ice concentration)), MAR(NorESM1-M) displays a negative
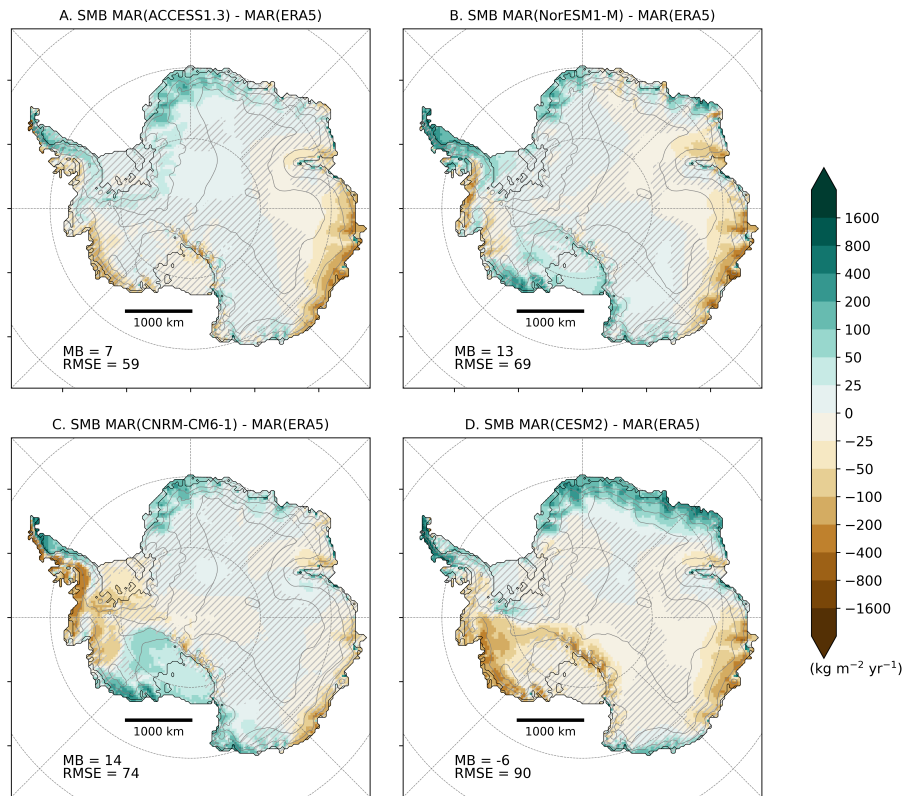
Figure 2. Comparison between the annual mean SMB simulated by MAR forced by ACCESS1.3 (A), NorESM1-M (B), CNRM-CM6-1 (C), CESM2 (D) and the annual mean SMB simulated by MAR(ERA5) ($\mathrm{kg\,m^{-2}\,yr^{-1}}$) over 1981–2010. Locations where anomalies are smaller than the (natural) interannual variability of the present climate (interannual standard deviation) are hatched.

temperature anomaly up to 3°C over the plateau despite reducing the negative anomaly over half of the Antarctic ice sheet to non-significant differences in summer (Fig. S3). This however leads to reduced surface melting (-72 Gt yr^{-1}).

MAR(CNRM-CM6-1) simulates nearly the same integrated snowfall amount as MAR(ERA5) but has a higher SMB RMSE due to a less accurate spatial representation of the precipitation. This results from an overestimation of the precipitable water combined to a higher mean sea level pressure in CNRM-CM6-1 potentially reducing cyclonic activity. MAR(CNRM-CM6-1) underestimates the SMB over the Ellsworth Land and the windward side of the Peninsula but overestimates it over Marie Byrd Land, Queen Maud Land and Victoria Land (Fig. 2). Agosta et al. (in preparation) revealed a strong negative temperature anomaly surrounding the ice sheet, yielding lower temperature in MAR(CNRM-CM6-1) compared to MAR(ERA5) over the plateau. However, these differences are non significant over the margins, the Ronne ice shelf excepted (Fig. S3).

As it simulates lower snowfall amounts than MAR(ERA5), MAR(CESM2) slightly underestimates the mean integrated SMB. However, MAR(CESM2) represents a stronger accumulation over the area between the Peninsula, Queen Maud Land and Enderby Land (Fig. 2). This results from the significant overestimation of the precipitable water and the sea level pressure

in CESM2 over this area. On the contrary, MAR(CESM2) simulates a lower accumulation over Wilkes Land and the Amundsen sector. CESM2 is colder than ERA5 but the difference is reduced in summer (Agosta et al., in preparation), leading to mostly non significant temperature anomalies in summer (Fig. S3) ..

220   In general, the SMB downscaled by MAR forced by the 4 ESMs is close to MAR(ERA5). The anomalies of the annual mean SMB are lower than the interannual variability of the SMB over the historical period. MAR(ACCESS1.3) has the best representation of the Antarctic SMB over the current climate (mean bias: -3 $\mathrm{Gt\,yr^{-1}}$, spatial rmse: 59 $\mathrm{kg\,m^{-2}\,yr^{-1}}$), while MAR(CESM2) is the least accurate (mean bias: -26 $\mathrm{Gt\,yr^{-1}}$, spatial rmse: 90 $\mathrm{kg\,m^{-2}\,yr^{-1}}$). The results of our experiments over the current climate are consistent with the ranking of the ESMs given by Agosta et al. (2015), Barthel et al. (2020), and

225   Agosta et al. (in preparation). This highlights the importance of selecting ESMs that correctly represent the historical climate (in particular the free atmosphere and the general circulation) around Antarctica as they induce biases in the downscaled near-surface climate independently of the capacity of the RCM to improve ESMs results. It is also important to note that the spatial and integrated anomalies are close to (or even lower than) the spread between several RCMs all forced by ERA-Interim (Mottram et al., 2020). This suggests a good ability of the different simulations to closely reproduce the SMB over the present

230   climate and gives some confidence in the results of the future projections..

4   Results

Our projections of the Antarctic SMB show a trend towards surface mass gains by the end of the 21st century (Fig. S5). MAR simulations forced by the high-emission scenarios ssp585 and RCP8.5 suggest a generally higher Antarctic SMB (including ice shelves) during 2071–2100 than for 1981–2010, with positive anomalies between +257 $\mathrm{Gt\,yr^{-1}}$ for MAR(CNRM-CM6-1)

235   and +505 $\mathrm{Gt\,yr^{-1}}$ for MAR(CESM2). The projections reveal a spread of 248 $\mathrm{Gt\,yr^{-1}}$, i.e., almost a factor two between the lowest and the highest increase in SMB. Such a high amplitude highlights the importance of using multiple models for a better assessment of the uncertainties when discussing the future state of the Antarctic SMB throughout the 21st century.

4.1   Regional changes

Using Antarctic-integrated values however hides two distinct signals. The diverging trajectories of SMB over grounded versus

240   floating ice (Fig. 3) suggest contrasting processes at play. In the rest of this manuscript, we will therefore discuss separately the ice shelves and the grounded ice sheet. This distinction is also justified by the direct equivalent between grounded-ice mass change and mean sea-level variations, whereas ice shelves do not directly contribute to sea-level variations even if their surface processes (such as hydrofracturing) are of crucial importance for the ice-sheet dynamics and therefore the Antarctic mass balance evolution. The locations mentioned hereafter are illustrated in Fig. S6.

245 ### 4.1.1   Grounded ice sheet

The grounded Antarctic SMB is projected to increase by +349 $\mathrm{Gt\,yr^{-1}}$ (MAR(NorESM1-M)) to +751 $\mathrm{Gt\,yr^{-1}}$ (MAR(CESM2)) from 1981–2010 to 2071–2100 (Table 1). Our simulations suggest large (up to more than twice the present - natural - inter-
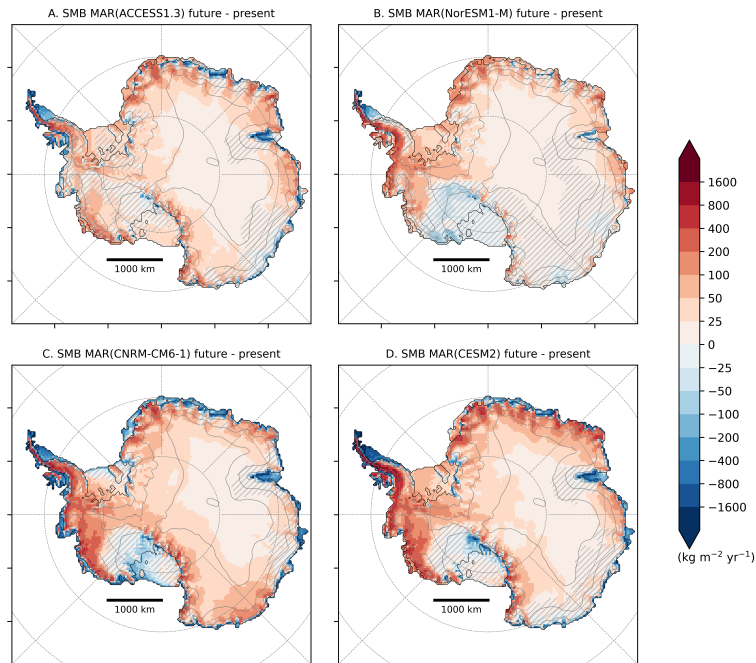
Figure 3. SMB changes $(\mathrm{kg\,m^{-2}\,yr^{-1}})$ between 2071–2100 and 1981–2010 as modelled by MAR forced by ACCESS1-3 (A), NorESM1-M (B), CNRM-CM6-1 (C), and CESM2 (D). Locations where future changes are smaller than the (natural) interannual variability over the present climate (interannual standard deviation) are hatched.

annual variability) positive SMB anomalies in West Antarctica (Marie Byrd and Ellsworth Land) and over the mountainous regions of the Antarctic Peninsula (Fig. 3). The situation in East Antarctica is more contrasted. The increase is significant (i.e, larger than the interannual variability over 1981–2010) in Queen Mary Land and high-elevation plateaus, while George V Land, Adelie Land and Wilkes Land are projected to have a weak increase in SMB for all the simulations, except MAR(CNRM-CM6-1) which suggests a strong increase there.

From 2015 onwards, the grounded SMB increases in all our MAR simulations (Fig. 5A). Large differences between projections appear around 2040–2050 when MAR(CESM2) and MAR(CNRM-CM6-1) suggest the strongest increase after 2050 and 2065 respectively while MAR(NorESM1-M) and MAR(ACCESS1.3) show a substantial increase at the end of the 21st century. Finally, only MAR(CNRM-CM6-1) suggests a SMB decrease beyond 2095.

The grounded SMB trend is mainly dominated by an increase in snowfall (Fig. 5B). Increased air moisture content associated to higher air temperatures leads to a widespread increase in snowfall over the AIS, explaining most of the positive SMB anomalies. This increase is stronger where air masses saturate as they adiabatically cool when rising with the topography (Agosta et al., 2013; Ligtenberg et al., 2013). Figure 4 shows that the largest increase occurs in West Antarctica, where the accumulation by snowfall already is the highest over the present climate. Although more snowfall can be expected over most of the AIS in a warmer climate (Palerme et al., 2017), some parts of the Antarctic grounded ice sheet show negative anomalies. This decrease
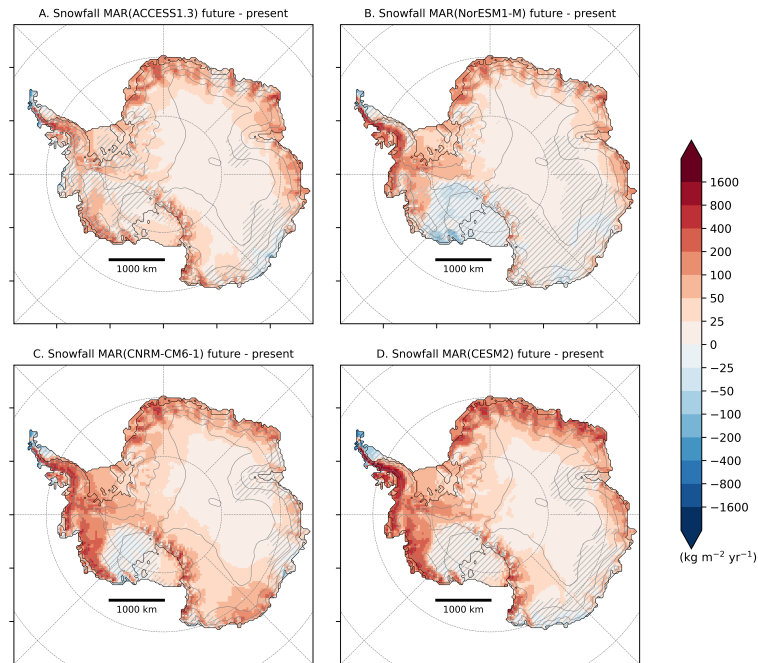
Figure 4. Snowfall changes $(\mathrm{kg\,m^{-2}\,yr^{-1}})$ between 2071–2100 and 1981–2010 as modelled by MAR forced by ACCESS1-3 (A), NorESM1-M (B), CNRM-CM6-1 (C), and CESM2 (D), using ssp585 and RCP8.5. Locations where changes are smaller than the (natural) interannual variability of the present climate (interannual standard deviation) are hatched.

in snowfall affects areas such as inland of Marie Byrd where the SMB consequently decreases. This strong snowfall increase over the peripheral slopes associated afterwards with an inland reduction could result from enhanced condensation over the marginal slopes reducing moisture intrusion and snowfall formation inland (Kittel et al., 2018). Although this effect may be present in our projections, Figure S7(b) also reveals a deepening of the Amundsen Sea Low enhancing moisture advection towards the Antarctic peninsula in MAR(NorESM1-M). This deepening projected by NorESM-M especially occurs in winter (Raphael et al., 2016) and result from rising greenhouse-gas emissions (Hosking et al., 2016; Raphael et al., 2016).

Snowfall increase in response to higher air temperatures also competes with a subsequent increase in runoff over the grounded ice margins (Fig. 5E). Although runoff amounts are negligible in the present climate and the increase in runoff is lower than the increase in snowfall, the future runoff contribution could compensate up to 34% of the snowfall increase in MAR(CNRM-CM6-1) over 2071–2100, questioning the use of Precipitation-Evaporation to compute SMB used in earlier studies (e.g., Palerme et al., 2017; Favier et al., 2017; Gorte et al., 2019). Other surface mass flux components such as rainfall (Fig. 5G), deposition and sublimation are not projected to contribute significantly to SMB changes.

From 1981 to 2100, our results suggest a grounded cumulative contribution of -3.7 cm, -5.8 cm, -8.1 cm and -10.6 cm SLE for MAR(NorESM1-M), MAR(ACCESS1.3), MAR(CNRM-CM6-1) and MAR(CESM2) respectively. Given that all these
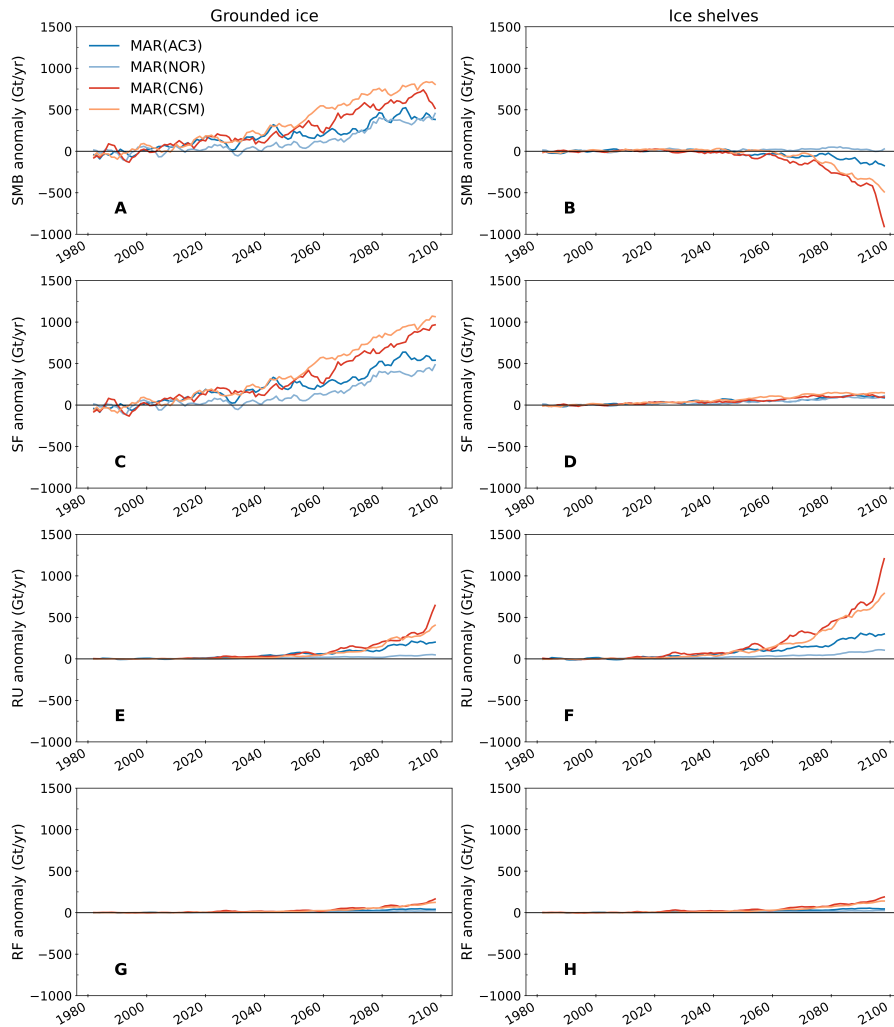
Figure 5. Time series of the integrated annual SMB (A, B), snowfall (C, D), runoff (E, F) and rainfall (G, H) anomalies ($\mathrm{Gt\,yr^{-1}}$) over the Antarctic grounded ice (A, C, E, G) and the Antarctic ice shelves (B, D, F, H) from 1980 to 2100 simulated by MAR forced by RCP8.5 or ssp585 scenarios from ACCESS1-3 (blue), NorESM1-M (light blue), CNRM-CM6-1 (red), and CESM2 (orange) compared to the 1981–2010 reference period. A running average of 5 years was applied to the original time series for better readability. Sublimation and surface melt changes are shown in Fig. S8.

projections are obtained from similar anthropogenic forcing, this demonstrates the necessity of using several ESMs to evaluate the Antarctic contribution to the sea-level rise in high-emission scenarios at the end of the 21st century.

4.1.2 Ice shelves

280 The SMB evolution over the ice shelves shows more uncertainties depending on the forcing ESM. It remains close to the present-day values in MAR(NorESM1-M), while it strongly decreases after 2075 in the other simulations (Fig. 5B). All the MAR simulations agree on a significant SMB decrease over the ice shelves on the lee side (eastern) of the Northern Antarctic Peninsula and near Amery's grounding line (Fig. 3). With the exception of MAR(NorESM1-M), our projections also suggest a strong SMB decrease over the ice shelves on the windward side of the Northern Peninsula and over a majority of the ice

285 shelves in Wilkes Land and in Queen Maud Land. Only MAR(CNRM-CM6-1) reveals widespread negative SMB anomalies over all the small Antarctic peripheral ice shelves. The Ronne-Filchner Ice Shelf is expected to have an increase in SMB, even in MAR(CNRM-CM6-1) except in the vicinity of the ocean. Our simulations suggest diverging responses over the Ross ice shelf, positive in MAR(ACCESS1.3) and MAR(CESM2), negative in MAR(CNRM-CM6-1) and MAR(NorESM1-M). The Ross ice shelf illustrates the large uncertainties related to the different model forcings on the future SMB over the Antarctic ice

290 shelves until 2100.

MAR suggests an increase in snowfall over ice shelves (between +83 $\mathrm{Gt\,yr^{-1}}$ and +139 $\mathrm{Gt\,yr^{-1}}$) regardless of the forcing ESM, but also a significant increase in rainfall (+18 $\mathrm{Gt\,yr^{-1}}$ to 108 $\mathrm{Gt\,yr^{-1}}$) (Table 1). The increase in snowfall over the ice shelves is however weaker than the increase over the grounded margins, suggesting a stronger saturation of air masses when lifted over the ice-sheet slope (Fig. 4). Over the period 2071–2100, rainfall anomalies can be as large as snowfall anomalies

295 on the ice shelves, or even outpace the increase in snowfall in MAR(CNRM-CM6-1), where snowfall is projected to decrease at the very end of the century (Fig. 5H). The warmer air also induces a conversion of snowfall into rainfall over the Antarctic Peninsula, where the total precipitation is projected to increase despite an increasing fraction falling as rain. Snowfall also decreases over the Ross Ice Shelf in MAR(NorESM1-M) due to a pronounced intensification of the Amundsen Sea Low system bringing more moisture towards the Peninsula and less over the Ross Ice Shelf (Fig. S7b), which reduces SMB over

300 this area.

Higher air temperature also causes a significant increase in surface melt. Repeated years of intense melting, combined with increased rainfall, reduce the firn air content and weaken the snowpack capacity to retain liquid water. This results in large runoff production rates over the ice shelves, except over the Ronne-Filchner due to its more southern position, as displayed in Fig. 6. MAR(NorESM1-M) suggests the lowest increase in runoff (+18 $\mathrm{Gt\,yr^{-1}}$), which is one order of magnitude lower than

305 for MAR(CNRM-CM6-1) (+558 $\mathrm{Gt\,yr^{-1}}$).

The amount of runoff projected at the end of the century explains the large changes in SMB over the ice shelves (Fig. 5F). The projected SMB decrease in MAR(CNRM-CM6-1) over the Ross ice shelf results from the larger increase in runoff than in snowfall while the decrease in SMB in the MAR(NorESM1-M) experiment is only attributed to reduced snowfall accumulation. Finally, the sharp runoff increase in MAR(CNRM-CM6-1) starting in 2090 reflects a widespread runoff over nearly all the ice

310 shelves (Fig. 6).
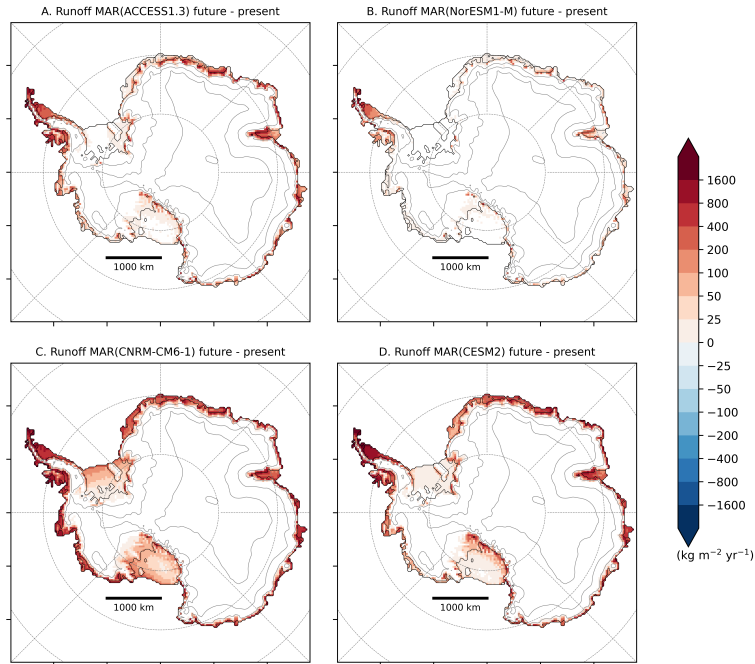
Figure 6. Changes in ruonff production $(\mathrm{kg\,m^{-2}\,yr^{-1}})$ between 2071–2100 and 1981–2010 as modelled by MAR forced by ACCESS1-3 (A), NorESM1-M (B), CNRM-CM6-1 (C), and CESM2 (D). Locations where changes are smaller than the (natural) interannual variability of the present climate (interannual standard deviation) are hatched.

Table 1. Integrated anomalies $(\mathrm{Gt\,yr^{-1}})$ of SMB, snowfall, rainfall, runoff, net sublimation (defined as surface sublimation minus surface deposition), and melt for the grounded ice sheet and the ice shelves over 2071–2100 compared to the present (1981–2010) from RCP8.5 and ssp585 simulations. All the anomalies are larger than the present interannual variability (i.e, standard deviation) of the same simulation and are therefore considered as significant.

	SMB	Snowfall	Rainfall	Runoff	Net sublimation	Melt
Grounded ice (11.94 10^6 km^2)						
MAR(ACCESS1.3)	+382 ± 75	+501 ± 96	+36 ± 5	+151 ± 44	+4 ± 3	+277 ± 69
MAR(NorESM1-M)	+349 ± 61	+367 ± 64	+18 ± 5	+32 ± 11	+4 ± 3	+79 ± 25
MAR(CNRM-CM6-1)	+598 ± 67	+753 ± 120	+85 ± 29	+260 ± 124	-20 ± 12	+490 ± 17
MAR(CESM2)	+751 ± 60	+880 ± 111	+75 ± 24	+221 ± 89	-17 ± 8	+395 ± 135
Ice shelves (1.77 10^6 km^2)						
MAR(ACCESS1.3)	-98 ± +44	+94 ± 17	+41 ± 9	+229 ± 62	+4 ± 1	+416 ± 93
MAR(NorESM1-M)	+30 ± 14	+83 ± 14	18 ± 15	+69 ± 23	+3 ± 1	+182 ± 51
MAR(CNRM-CM6-1)	-335 ± 190	+109 ± 12	+108 ± 34	+558 ± 227	-6 ± 4	+781 ± 220
MAR(CESM2)	-240 ± 127	+139 ± 8	+90 ± 28	+476 ± 162	-7 ± 3	+703 ± 179

4.2 Links with the ESM near-surface temperature

Our projections of the 21st century evolution of the Antarctic SMB yield large spread in SMB for both the Antarctic grounded ice and ice shelves. This spread can mostly be attributed to different warming rates in the forcing ESM, as they show a broad range of warming rates despite a similar radiative forcing due to anthropogenic emissions (Figure 1).

We identify the 30-year periods (different for each ESM) characterised by an Antarctic (90°S–60°S) annual near-surface climate about +2.5°C warmer on average than the climate over the historical period (1981–2010) to compare SMB anomalies resulting from an equivalent warming. This +2.5°C warming corresponds to the strongest 30-year averaged near-surface warming common to all our selected ESMs. The period selected for each ESM is listed in Table S4. Mean SMB anomalies projected by MAR during these periods reveal a very similar spatial pattern between all our experiment. A +2.5°C warming yields a mostly non-significant increase in SMB over the grounded ice sheet and a weak (negative) change over the surrounding ice shelves (Fig. S9). This comparison at equivalent warming but different 30-year periods shows that the spread in the future SMB is mainly due to the timing and magnitude of the warming projected by the ESMs.

To remove the uncertainty associated to the different warming rates, we associate the future annual anomalies modelled by MAR to annual near-surface temperature anomalies over 90°S–60°S from the forcing ESM. Figure 7 reveals more consistent projections between all our experiments. Note that associating annual MAR anomalies with ESM temperature anomalies in the free atmosphere (700 or 850 hPa) does not change the comparison (not shown).

Precipitation increases following the Clausius-Clapeyron relation, a weak exponential form that can be approximated as a (nearly) linear relationship for moderate warming over the AIS (Agosta et al., 2013; Frieler et al., 2015; Palerme et al., 2017). The grounded (Fig. S10A) increase is dominated by snowfall anomalies (Fig. 7A) with a weak contribution of rainfall (Fig. 7C). Over the ice shelves, snowfall is no longer increasing for strong warmings above +7.5°C. A the total increase in precipitation remains also approximately linear (Fig. S10B), an increasing proportion of the potential additional precipitation falls as rain instead of snow for higher temperature over the ice shelves. Under increasing warming, more locations will experience rainfall, melting and runoff. We therefore link rainfall (Fig. 7C,D) and runoff (Fig. 7E,F) anomalies with near-surface temperature anomalies using a quadratic relation reflecting postive feedbacks (Fettweis et al., 2013). Our results suggest that the increase in rainfall will be stronger than the snowfall increase over the ice shelves for warming above 7.5°C. The integrated increase in runoff is stronger over ice shelves than over the grounded ice, despite lower floating areas. This is mainly explained by the low surface elevation of the ice shelves. Other studies (e.g., Kuipers Munneke et al., 2014; Trusel et al., 2015; Donat-Magnin et al., 2020) also linked an exponential increase in melting with air temperature over the AIS.

Although the dominant signal explaining grounded SMB variations is the snowfall increase, the trend suggest a slowing or even a lower grounded SMB increase for warmings higher than +7.5°C (Fig. 8). This results from a strong increase in the grounded ice-sheet runoff. However, this grounded-SMB threshold is only supported by MAR(CNRM-CM6-1). Since this warming magnitude is not reached across all our other projections and as CNRM-CM6-1 is the warmest model in the entire CMIP5 and CMIP6 database, it would require longer projections to confirm the confidence of this threshold.

Over the ice shelves, a near-surface temperature increase by more than +2°C results in runoff anomalies larger than precipitation anomalies, hence leading to negative SMB anomalies (Fig. 8). While ice-shelf collapses could already occur due to hydrofracturing caused by enhanced surface melt, additional warming beyond this threshold will result in less surface accumulation, or even ice-shelf thinning for the warmings that result in a SMB decrease stronger than 478 $\mathrm{Gt\,yr^{-1}}$ (i.e., the present SMB simulated by MAR(ERA5)) over the ice shelves). This might induce marine ice-sheet instability and/or enhancing positive feedbacks between ice dynamics and new damage weakening the ice shelves (Lhermitte et al., 2020).

5   Discussion

5.1   Statistical projections for the CMIP5 and CMIP6 ensemble

Anomalies in Antarctic SMB and its driving components (precipitation and runoff) are strongly explained by near-surface ESM temperature anomalies between 90°S–60°S as discussed above (see Sect. 4.2). We therefore propose to reconstruct the SMB for both the Antarctic grounded ice (Eq. 2) and ice shelves (Eq. 3) using ESM near-surface temperature anomalies:

$$\Delta SMB_{grd} \approx -1.3\,\Delta TAS_{90-60S}^2 + 115.4\,\Delta TAS_{90-60S} - 11.1, \tag{2}$$

$$\Delta SMB_{shf} \approx -12.7\,\Delta TAS_{90-60S}^2 + 32.1\,\Delta TAS_{90-60S} - 3.1, \tag{3}$$

where ΔSMB_{grd}, ΔSMB_{shf}, and ΔTAS_{90-60S} represent the SMB anomalies over the grounded ice and ice shelves (in $\mathrm{Gt\,yr^{-1}}$), and the ESM 90°S–60°S near-surface temperature anomaly (in °C) compared to their respective mean value over 1981–2010. A more detailed description of the ability of this regression to represent SMB anomalies is presented in Supplementary Material (Fig S11). Since CNRM-CM6-1 has the strongest Antarctic near-surface warming among all CMIP5 and CMIP6 models, we can use this regression to predict the future SMB in 2100 without any extrapolation outside the warming range of our projections. However, this implies several hypotheses, such as the absence of strong atmospheric circulation changes (influencing humidity advection) or a fixed ice surface (topography).

Using Eq. (2) and Eq. (3), we reconstructed the annual Antarctic SMB for all the CMIP5 (RCP8.5) and CMIP6 (ssp126, ssp245, ssp585) models for which the annual near-surface temperature is available until 2100. The projected SMB anomalies remain similar until 2040–2050 in all the reconstructions. They then start to diverge and lead to a difference of -1.2cm SLE (-6.3 ± 2.0 cm SLE in CMIP6-ssp585 vs -5.1 ± 1.9 cm in CMIP5-RCP8.5 summed over the period 1981–2100). From the period 2045–2050, the SMB on the ice shelves starts decreasing in CMIP5-RCP8.5 models, and even more in CMIP6-ssp585 models, with a multi-model-mean difference of 65 $\mathrm{Gt\,yr^{-1}}$ over 2071–2100. A few models nonetheless suggest a steady-state ice-shelf SMB both in the CMIP5 and CMIP6 ensembles. It should also be noted that the CMIP6-ssp585 spread is much larger than in CMIP5-RCP8.5, as it ranges from strong negative anomalies (-600 $\mathrm{Gt\,yr^{-1}}$, i.e. lower than present ice-shelf SMB) to steady state or even slightly positive anomalies on the ice shelves. The CMIP6-ssp585 ensemble-mean value in 2100 is also nearly outside the spread range of CMIP5-RCP8.5 models highlighting the average stronger SMB decrease in CMIP6-ssp585. Similarly to what is projected for the Greenland ice sheet (Hofer et al., 2020)), the higher equilibrium climate sensitivity of
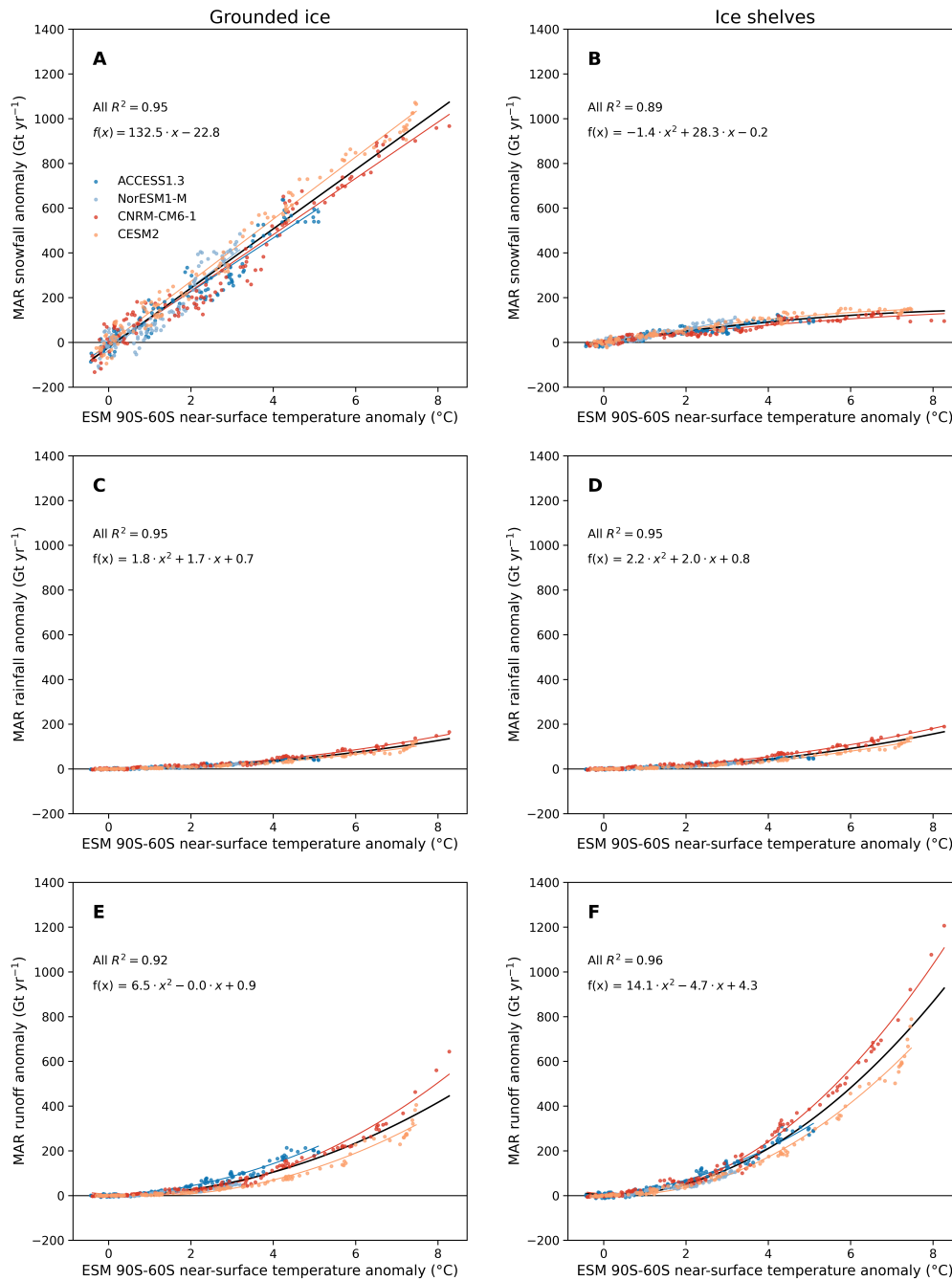
Figure 7. MAR snowfall (A, B), rainfall (C, D) and runoff (E, H) anomalies ($\mathrm{Gt\,yr^{-1}}$) over the grounded ice (A, C, E) and ice shelves (B, D, H) compared to the annual near-surface temperature anomaly from the forcing ESM between 90°S-60°S (°C). The black regression was computed using all the MAR-ESM anomalies while individual regression are also represented (coloured lines). The regression equation and determination coefficient are mentioned for each scatter plot.
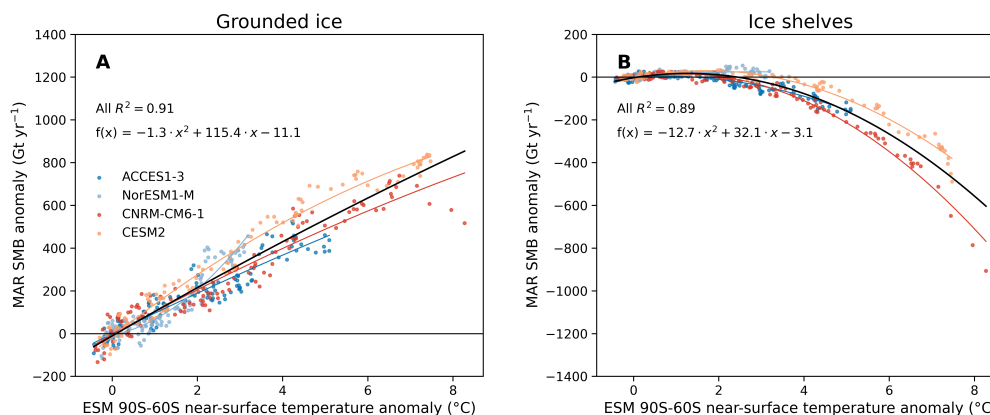
Figure 8. MAR SMB anomaly over the grounded ice (A) and ice shelves (B) compared to the annual near-surface temperature anomaly from the forcing ESM between 90°S-60°S (°C). The black regression was computed using all the MAR-ESM anomalies while individual regression are also represented (coloured lines).

several CMIP6 models largely explains the differences between the CMIP5 and CMIP6 results. Both the CMIP6-ssp126 and CMIP6-ssp245 scenarios yield a stable SMB (increased over the grounded ice and close to steady state to slightly negative over the ice shelves) after 2050. In cumulative terms, our CMIP6 reconstructions of summed anomalies over the 21st century indicate Antarctic grounded-surface contributions of -3.0 $\pm$1.4 cm SLE for CMIP6-ssp126 and -4.2 $\pm$1.6 cm SLE for CMIP6-ssp245, i.e a lower sea-level rise mitigation than for CMPIP6-ssp585. As described in Sect. 4, a high temperature increase induces higher precipitation rates but also higher runoff over the grounded ice sheet. Figure S12 reveals large spreads in both integrated snowfall and runoff changes. However, as runoff increase partly compensates snowfall increase, the spread in SMB change is strongly reduced compared to the individual components. Note that the uncertainties associated to mean reconstituted anomalies are only based on the intermodel variability over both the grounded ice sheet and the ice shelves but the uncertainties would have been larger if the biases of MAR (over current climate) and our regressions (Eq. (2) and Eq. (3)) were taken into account.

5.2 Comparison with the ISMIP6-derived SMB

Due to time constraints and computational demands faced by the Ice Sheet Model Intercomparison Project (ISMIP6, Nowicki et al., 2016), future Antarctic projections for forcing ice-sheet models were derived directly from ESMs while, over the Greenland ice sheet MAR was used to downscale ESM projections (Nowicki et al., 2020). However, using ESMs to study the evolution of the SMB often involves several compromises related to their coarse resolution and their low sophistication to represent important physical processes of polar regions. Some studies have argued that RCMs add uncertainties in the down-scaling product (Nowicki et al., 2016), but the significant SMB biases in ESMs over the current climate (e.g., Krinner et al., 2007; Agosta et al., 2015; Lenaerts et al., 2017b; Palerme et al., 2017; Krinner and Flanner, 2018) might be a larger source
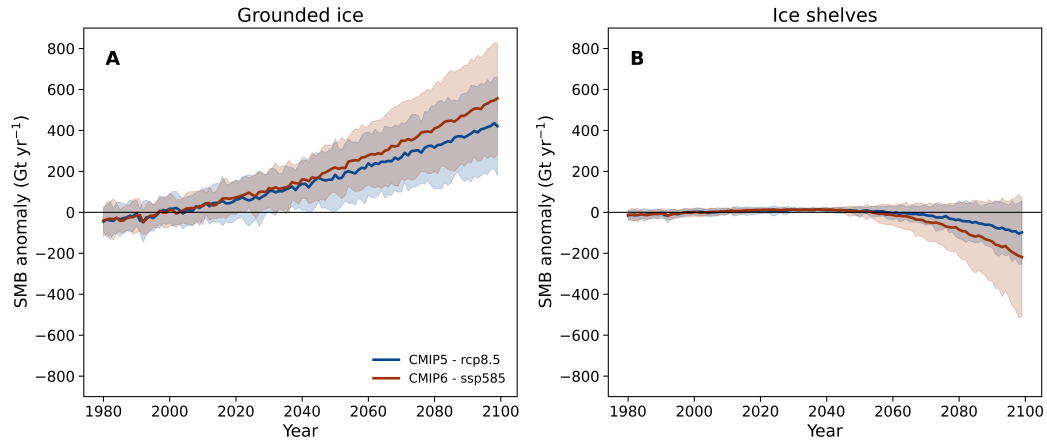
Figure 9. Reconstructed SMB anomaly $\mathrm{Gt\,yr^{-1}}$ using CMIP5-RCP8.5 (blue) and CMIP6-ssp585 models (red) over the Antarctic grounded ice (A) and ice shelves (B). Projections are shown using the multi-model mean (solid lines) and the 5 to 95% range, corresponding to ±1.64 standard deviation, across the distribution of individual models (shading).
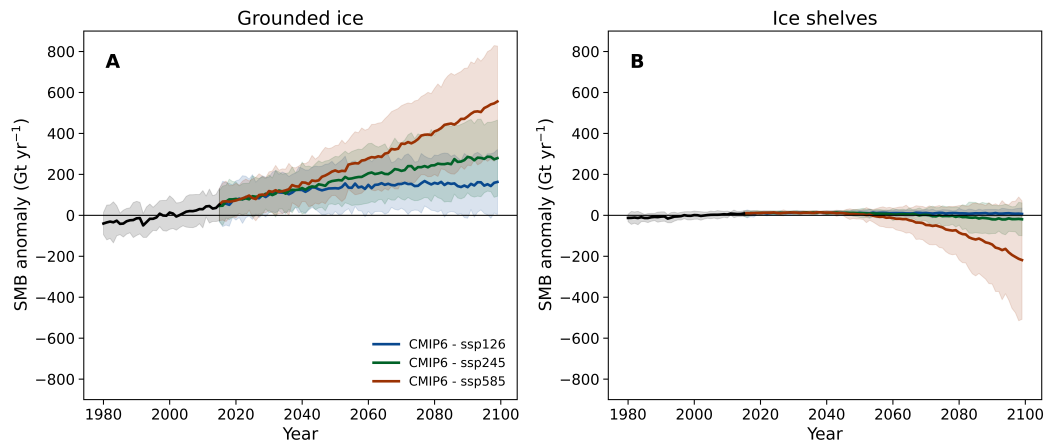
Figure 10. Reconstructed SMB anomaly $\mathrm{Gt\,yr^{-1}}$ for the CMIP6 models using the ssp126 (green), ssp245 (green) and ssp585 (red) scenarios over the Antarctic grounded ice (A) and ice shelves (B). Projections are shown using the multi-model mean (solid lines) and the 5 to 95% range, corresponding to ±1.64 standard deviation, across the distribution of individual models (shading).
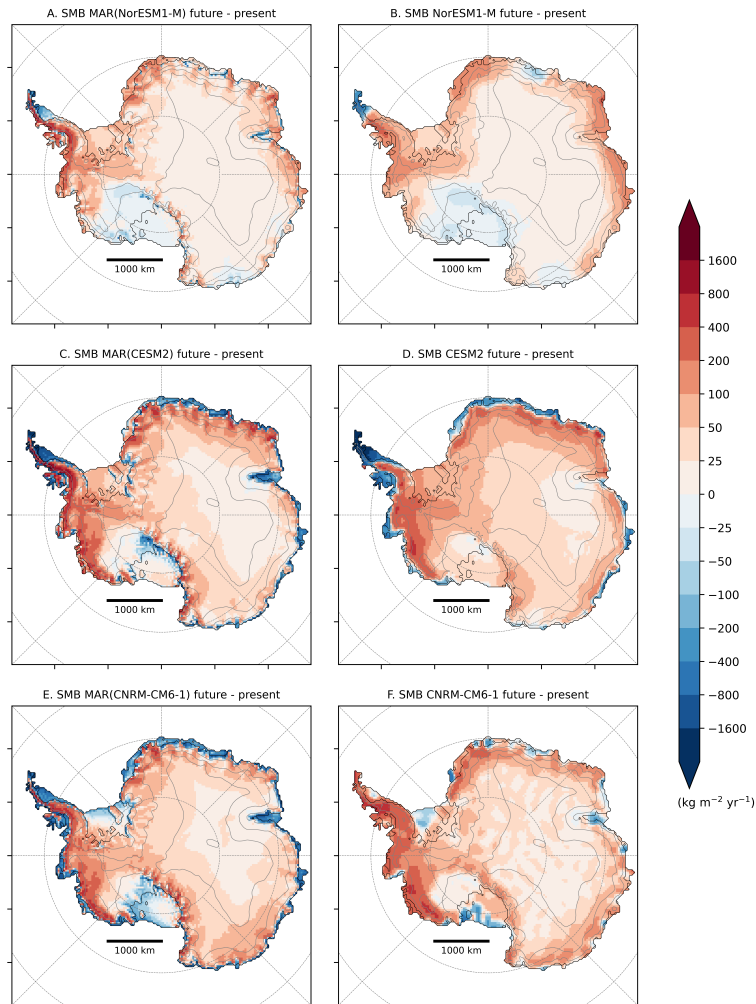
Figure 11. Comprison between SMB anomalies between 2081–2100 and 1995–2014 ($\mathrm{kg\,m^{-2}\,yr^{-1}}$) projected by MAR forced by NorESM1-M (A), CESM2(C), CNRM-CM6-1 (E), and the ISMIP6-SMB directly derived from NorESM1-M (B), CESM2 (D) and CNRM-CM6-1 (F).

of uncertainties than the downscaling itself. Therefore, we compare our MAR projections forced by NorESM1-M (RCP8.5),
395   CESM2 and CNRM-CM6-1 (ssp585) to the ISMIP6-derived SMB used to predict the future Antarctic sea-level contribution
(Seroussi et al., 2020) by interpolating the 32 km SMB fields built by ISMIP6 on the 35 km MAR grid.

    Figure 11 compares future SMB changes (2081–2100 versus 1995–2014 i.e., the ISMIP6 reference period) projected by
MAR and the respective forcing ESMs. While the MAR projections are relatively insensitive to the forcing ESM for the
same warming (see Sect. 4.2), the comparison between MAR and the forcing ESM reveals large differences, independently of
400   the differences due to the higher resolution used in MAR that enables to distinguish high-elevation positives anomalies from
low-elevation negative anomalies. For example, CNRM-CM6-1 projects a strong near-surface Antarctic warming (Fig. 1 and
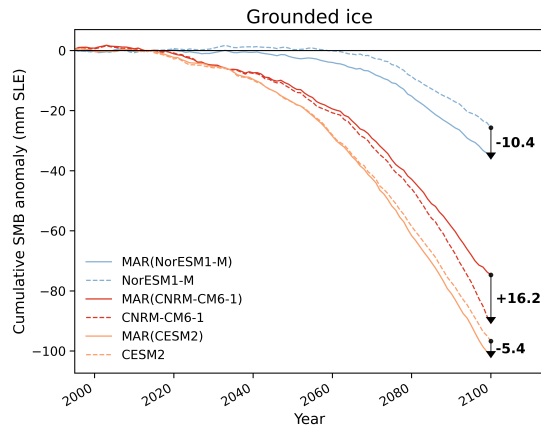
Figure 12. Cumulative contribution of the grounded Antarctic SMB (mmSLE) of MAR forced by NorESM1-M, CNRM-CM6-1, and CESM2 (solid ligne), and the ISMIP6-SMB directly computed from NorESM1-M, CNRM-CM6-1, and CESM2 (dashed lines) over 1995–2100. The differences between the cumulative contributions of the MAR experiments and their forcing ESM is also indicated in the figure.

Nowicki et al. (2020), Fig. 1a) but the related runoff increase is particularly weak (Fig. S13), leading to only very slightly negative anomalies, in contrast to MAR(CNRM-CM6-1), which simulates widespread negatives anomalies around nearly all the peripheral ice shelves consistent with a stronger warming 7. As highlighted by Fettweis et al. (2020), this suggests that the physics of the models and/or the biases over the current climate (in particular for the melt) could strongly influence the projected near-surface changes for identical changes in the free atmosphere. These MAR and ESM differences also highlight the importance of correctly representing the current climate and the need of additional projections relying on more models, including both RCMs and ESMs. As the integrated differences summed over 1995–2100 can be larger or as large as the differences between CMIP5-RCP8.5 and CMIP6-ssp585, or between CMIP6-ssp126 and CMIP6-ssp245 (Fig. 12), this also raises the question of the sensitivity to the forcing of ISMIP6 projections, where the SMB is used as an input for performing projections of the total AIS mass balance (Seroussi et al., 2020).

5.3 Limitations

Our projections suggest a significant ablation by runoff as the firn would not absorb all the additional liquid water, whereas almost all surface meltwater refreezes in the snowpack. MAR does not include a liquid-water routing scheme that could either create liquid-water flowing over the ice surface, or accumulate melted water into surface or sub-surface lakes, further away than the place of its production. The current view suggests that enhanced melt will be stored in crevasses or ponds that weaken ice shelves, potentially leading to their collapses by hydrofracturing (Scambos et al., 2000; Vieli et al., 2007; Pattyn et al., 2018). However, in some conditions, streams and rivers can transfer surface meltwater laterally and export it into the ocean (Kingslake et al., 2017; Pattyn et al., 2018; Dell et al., 2020; Arthur et al., 2020), which might eventually reduce the risk of hydrofracturing (Bell et al., 2017). Lake formation and meltwater runoff therefore represent a large uncertainty about the future

of the ice shelves and the contribution of the AIS to sea level. These processes have yet to be implemented in the snowpack module of MAR.

MAR is not coupled to an ice-sheet model in these simulations and therefore has a static ice-sheet geometry (ie., fixed surface elevation and ice/ocean mask) that could lead to biases in the simulated SMB. For instance, melt-elevation feedback due to the lowering of the surface elevation by atmospheric and basal melt are not taken into account with a fixed geometry. Hence, we probably underestimate surface melt rates by overestimating the future surface elevation (Ritz et al., 2015). Since the ice/ocean mask is fixed over the whole simulation period (1975–2100), integrated anomalies could also be biased. The ice-shelf area and associated negative SMB value are potentially overestimated due to the absence of collapse processes. In the same way, the extent of grounded ice is reduced as grounding lines retreat, which should induce a negative contribution of the surface to sea-level rise. These two implicit consequences of using fixed ice mask and elevation could partly compensate each other. The elevation feedback has been shown to matter for 21st century Greenland projections (Le clec'h et al., 2019), but its importance for the AIS remains an open question.

Our simulations also do not include drifting snow, which can be active up to 81% of the time in some locations (Amory, 2020). Drifting snow has been simulated as the main present ablation component of the Antarctic ice sheet (Lenaerts and Van den Broeke, 2012; Van Wessem et al., 2018) and can lead to exposure of low-albedo and blue-ice area (Lenaerts et al., 2017a). The sublimation of eroded particles also cools the atmosphere (Le Toumelin et al., 2020(in preperation)) and has a significant influence on the humidity budget of the near-surface atmosphere (Amory and Kittel, 2019). The drifting-snow scheme of MAR had not yet been evaluated at the scale of the ice sheet when we performed our simulations and was therefore deactivated. Projected runoff ablation is much higher than present wind-driven ablation suggesting that drifting snow would not remain the main ablation process by 2100. This highlights the importance of assessing the future Antarctic drifting-snow climate in the global warming context.

6   Conclusions

In this study, we use the regional atmospheric model MAR, which includes determinant polar surface physics, forced by four carefully-selected ESMs (ACCESS1.3, NorESM1-M, CNRM-CM6-1, CESM2) to study the future evolution of the Antarctic SMB. These CMIP5 and CMIP6 models projects a wide range of Antarctic near-surface warming (+3.2°C to +8.5°C) and enable us to investigate the AIS sensitivity to different warmer climates in 2100.

Our results reveal an increase in grounded SMB (+382 $\mathrm{Gt\,yr^{-1}}$ to +751 $\mathrm{Gt\,yr^{-1}}$) between 1981–2010 and 2071–2100 due to an increase in snowfall amounts, despite higher runoff values partly offset this increase (up to 34%). Higher surface meltwater production over the ice shelves at the end of the 21st century prevents a total absorption of additional liquid water by the snowpack, leading to high runoff values and mostly negative SMB anomalies. The spread over the ice shelves is however large, since our simulations project relatively stable SMB anomalies (+28 $\mathrm{Gt\,yr^{-1}}$) to strong negative anomalies (-335 $\mathrm{Gt\,yr^{-1}}$). Our results suggest significant differences at the end of the century at the scale of the entire ice sheet, whether we consider the

grounded ice or ice shelves. However, future spatial and integrated changes for a same warming are similar, suggesting than uncertainties are mainly due to the sensitivity of ESMs to anthropogenic forcing and the timing of the projected warming.

455 Future changes modelled by MAR are strongly correlated with the near-surface warming of the forcing ESMs around the AIS. Using a statistical regression, we reconstruct integrated SMB anomalies over the grounded ice sheet as well as over the ice shelves for the whole CMIP5 (RCP8.5) and CMIP6 (ssp126, ssp245, ssp585) database. Over 2071–2100 compared to the present, this reconstructed grounded SMB suggests a higher increase for CMIP6-ssp585 (+447 $\pm$ 134 Gt yr^{-1}) than for CMIP5-RCP8.5 (+ 353 $\pm$ 114 Gt yr^{-1}) that respectively corresponds to a 2000-2100 summed sea-level contribution of -6.3

460 $\pm$2.0 cm SLE and -5.1 $\pm$1.9 cm SLE. Low (ssp126) and intermediate (ssp245) CMIP6 emission scenarios project a lower negative contribution to sea-level rise than ssp585 (-3.0 $\pm$1.4 cm SLE using ssp126 and -4.2 $\pm$1.6 cm SLE using ssp245. Conversely, CMIP6-ssp585 yield a stronger SMB decrease over the ice shelves (-119 $\pm$ 100 Gt yr^{-1}) than CMIP5-RCP8.5 (-54 $\pm$ 55 Gt yr^{-1}).

Future SMB estimates are also used as forcing for ice-sheet models, notably in the ISMIP6 project, where SMB estimates

465 are directly derived from ESMs. Despite several improvements in the latest generation of CMIP6 ESMs, using these models to study the evolution of the SMB involves several compromises that could lead to large uncertainties in the future SMB. We therefore compare the MAR projected SMB to the ISMIP6-derived SMB, revealing large local and integrated differences between MAR and the respective forcing ESM. These MAR and ESM differences highlight the importance of correctly representing the current climate and the need of additional projections relying on more models including both RCMs and ESMs.

470 Although other processes such as basal melting of ice shelves could lead to their disappearance (Holland et al., 2019; Seroussi et al., 2020), increasing surface melt should remain weak, limiting potential ice-shelf collapses due to hydrofracturing under the Paris Agreement (limiting global warming to +1.5°C compared to pre-industrial temperature, which is a colder target than the projected mean CMIP6-ssp126 warming). This weak increase in melt amounts should also limit surface thinning and then positive feedbacks between surface damages and ice-shelf instability. However, large uncertainties remain in the influence

475 of surface melt on the ice-shelf stability. Furthermore, our results highlight a warming threshold (+2.5°C) where the ice-shelf SMB could decrease, suggesting a low range of warming before potential irreversible damages on the ice-shelves. Finally, our simulations also suggest a stabilisation or even a decrease in grounded SMB with a +7.5°C near-surface warming, which would lead to a decrease in the sea-level mitigation capacity of the grounded AIS surface. This warming is however reached before 2100 by only one model in the highest-emission scenario suggesting that more work is needed to asses the confidence of this

480 threshold, the response of the AIS surface to strong warming after 2100 and AIS contribution to global sea-level rise.

Code and data availability. The MAR code used in this study is tagged as v3.11.1 on https://gitlab.com/Mar-Group/MARv3.7. See http://www.mar.cnrs.fr for more information about downloading MAR. The MAR outputs used in this study are available on zenodo (doi:10.5281/zenodo.4459259) Other higher-frequency MAR results and python scripts are also available upon request by email (ckittel@uliege.be).

Author contributions. CK, CAm, and XF designed the study. CK ran the simulations, made the plots (benefiting from some CAg and SH's scripts), performed the analysis and wrote the manuscript. CAm, CAg, NJ and XF provided importance guidance while all the authors discussed and revised the manuscript.

Competing interests. The authors declare that they have no conflict of interest.

Acknowledgements. We acknowledge the World Climate Research Programme's Working Group on Coupled Modelling, which is responsible for CMIP, and we thank the climate modelling groups for producing their model output and making it available. We also acknowledge ISMIP6 for making its datasets available. We appreciate the support of the University of Wisconsin-Madison Automatic Weather Station Program for the data set, data display, and information, NSF grant number 1924730, as well as all the institutes that collected data over the ice sheet.

Computational resources have been provided by the Consortium des Équipements de Calcul Intensif (CÉCI), funded by the Fonds de la Recherche Scientifique de Belgique (F.R.S. – FNRS) under grant no. 2.5020.11 and the Tier-1 supercomputer (Zenobe) of the Fédération Wallonie Bruxelles infrastructure funded by the Walloon Region under grant agreement no. 1117545. This work was supported by the Fonds de la Recherche Scientifique – FNRS under grant no. T.0002.16.

References

Agosta, C., Favier, V., Krinner, G., Gallée, H., Fettweis, X., and Genthon, C.: High-resolution modelling of the Antarctic surface mass balance, application for the twentieth, twenty first and twenty second centuries, Climate dynamics, 41, 3247–3260, 2013.

Agosta, C., Fettweis, X., and Datta, R.: Evaluation of the CMIP5 models in the aim of regional modelling of the Antarctic surface mass balance, Cryosphere, 9, 2311–2321, https://doi.org/10.5194/tc-9-2311-2015, 2015.

Agosta, C., Amory, C., Kittel, C., Orsi, A., Favier, V., Gallée, H., van den Broeke, M. R., Lenaerts, J., van Wessem, J. M., van de Berg, W. J., et al.: Estimation of the Antarctic surface mass balance using the regional climate model MAR (1979-2015) and identification of dominant processes, Cryosphere, 13, 281–296, 2019.

Amory, C.: Drifting-snow statistics from multiple-year autonomous measurements in Adélie Land, East Antarctica, The Cryosphere, 14, 1713–1725, 2020.

Amory, C. and Kittel, C.: Brief communication: Rare ambient saturation during drifting snow occurrences at a coastal location of East Antarctica., The Cryosphere, 13, 2019.

Amory, C., Trouvilliez, A., Gallée, H., Favier, V., Naaim-Bouvet, F., Genthon, C., Agosta, C., Piard, L., and Bellot, H.: Comparison between observed and simulated aeolian snow mass fluxes in Adélie Land, East Antarctica, The Cryosphere, 9, 1373–1383, https://doi.org/10.5194/tc-9-1373-2015, 2015.

Amory, C., Kittel, C., Le Toumelin, Louis and, A. C., Favier, V., and Fettweis, X.: Performance of MAR (v3.11) at simulating the drifitng-snow climate and surface mass balance of Adelie Land, East Antarctica, will be submitted to Geoscientific Model Development, 2020(in preperation).

Arthur, J. F., Stokes, C., Jamieson, S. S., Carr, J. R., and Leeson, A. A.: Recent understanding of Antarctic supraglacial lakes using satellite remote sensing, Progress in Physical Geography: Earth and Environment, p. 0309133320916114, 2020.

Barthel, A., Agosta, C., Little, C. M., Hattermann, T., Jourdain, N. N., Goelzer, H., Nowicki, S., Seroussi, H., Straneo, F., and Bracegirdle, T. T.: CMIP5 model selection for ISMIP6 ice sheet model forcing: Greenland and Antarctica, Cryosphere, 14, 855–879, 2020.

Bell, R. E., Chu, W., Kingslake, J., Das, I., Tedesco, M., Tinto, K. J., Zappa, C. J., Frezzotti, M., Boghosian, A., and Lee, W. S.: Antarctic ice shelf potentially stabilized by export of meltwater in surface river, Nature, 544, 344–348, 2017.

Bentsen, M., Bethke, I., Debernard, J. B., Iversen, T., Kirkevåg, A., Seland, Ø., Drange, H., Roelandt, C., Seierstad, I. A., Hoose, C., et al.: The Norwegian earth system model, NorESM1-M—Part 1: Description and basic evaluation of the physical climate, Geoscientific Model Development, 6, 687–720, 2013.

Bi, D., Dix, M., Marsland, S. J., O'Farrell, S., Rashid, H., Uotila, P., Hirst, A. C., Kowalczyk, E., Golebiewski, M., Sullivan, A., et al.: The ACCESS coupled model: description, control climate and evaluation, Aust. Meteorol. Oceanogr. J, 63, 41–64, 2013.

Brun, E., David, P., Subul, M., and Brunot, G.: A numerical model to simulate snow-cover stratigraphy for operational avalanche forecasting, Journal of Glaciology, 38, 13–22, 1992.

Danabasoglu, G., Lamarque, J.-F., Bacmeister, J., Bailey, D., DuVivier, A., Edwards, J., Emmons, L., Fasullo, J., Garcia, R., Gettelman, A., Hannay, C., Holland, M., Large, W. G., Lauritzen, P. H., Lawrence, D. M., Lenaerts, J. T. M., Lindsay, K., Liscomb, W. H., Mills, M. J., Neale, R., Oleson, K. W., Otto-Bliesner, B., Philips, A. S., Sacks, W., Tilmes, S., van Kampenhout, L., Vertenstein, M., Bertini, A., Dennis, J., Deser, C., Fischer, C., Fox-Kemper, B., Kay, J E dand Kinnison, D., Kushner, P. J., Larson, V. E., Long, M. C., Mickelson, S., Moore, J. K., Nienhouse, E., Polvani, L., Rasch, J., and Strand, W. G.: The Community Earth System Model version 2 (CESM2), Journal of Advances in Modeling Earth Systems, 12, e2019MS001 916, 2020.

De Ridder, K. and Gallée, H.: Land surface-induce regional climate change in Southern Israel, Journal of Applied Meteorology, 37, 1470–1485, 1998.

De Ridder, K. and Schayes, G.: The IAGL Land Surface Model, Journal of Applied Meteorology, 36, 167–182, https://doi.org/10.1086/451461, 1997.

Delhasse, A., Kittel, C., Amory, C., Hofer, S., and Fettweis, X.: Brief communication: Interest of a regional climate model against ERA5 to simulate the near-surface climate of the Greenland ice sheet, The Cryosphere Discussions, 2019.

Dell, R., Arnold, N., Willis, I., Banwell, A., Williamson, A., Pritchard, H., and Orr, A.: Lateral meltwater transfer across an Antarctic ice shelf, The Cryosphere, 14, 2313–2330, 2020.

Dix, M., Vohralik, P., Bi, D., Rashid, H., Marsland, S., O'Farrell, S., Uotila, P., Hirst, T., Kowalczyk, E., Sullivan, A., Hailin, Y., Franklin, C., Sun, Z., Watterson, I., Collier, M., Noonan, J., Rotstayn, L., Steven, L., Uhe, P., and Puri, K.: The ACCESS coupled model: documentation of core CMIP5 simulations and initial results, Aust. Meteorol. Oceanogr. J, 63, 83–99, 2013.

Donat-Magnin, M., Jourdain, N. C., Kittel, C., Agosta, C., Amory, C., Gallée, H., Krinner, G., and Chekki, M.: Future ice-sheet surface mass balance and melting in the Amundsen region, West Antarctica, The Cryosphere Discussions, 2020, 1–30, https://doi.org/10.5194/tc-2020-113, https://tc.copernicus.org/preprints/tc-2020-113/, 2020.

Dupont, T. and Alley, R. B.: Assessment of the importance of ice-shelf buttressing to ice-sheet flow, Geophysical Research Letters, 32, 2005.

Eyring, V., Bony, S., Meehl, G. A., Senior, C. A., Stevens, B., Stouffer, R. J., and Taylor, K. E.: Overview of the Coupled Model Intercomparison Project Phase 6 (CMIP6) experimental design and organization, Geoscientific Model Development, 9, 1937–1958, 2016.

Favier, V., Krinner, G., Amory, C., Gallée, H., Beaumet, J., and Agosta, C.: Antarctica-regional climate and surface mass budget, Current Climate Change Reports, 3, 303–315, 2017.

Fettweis, X., Franco, B., Tedesco, M., Van Angelen, J., Lenaerts, J. T., van den Broeke, M. R., and Gallée, H.: Estimating the Greenland ice sheet surface mass balance contribution to future sea level rise using the regional atmospheric climate model MAR, The Cryosphere, 7, 469–489, 2013.

Fettweis, X., Box, J., Agosta, C., Amory, C., Kittel, C., Lang, C., van As, D., Machguth, H., and Gallée, H.: Reconstructions of the 1900–2015 Greenland ice sheet surface mass balance using the regional climate MAR model, Cryosphere, 11, 1015–1033, 2017.

Fettweis, X., Hofer, S., Krebs-Kanzow, U., Amory, C., Aoki, T., Berends, C. J., Born, A., Box, J. E., Delhasse, A., Fujita, K., Gierz, P., Goelzer, H., Hanna, E., Hashimoto, A., Huybrechts, P., Kapsch, M.-L., King, M. D., Kittel, C., Lang, C., Langen, P. L., Lenaerts, J. T. M., Liston, G. E., Lohmann, G., Mernild, S. H., Mikolajewicz, U., Modali, K., Mottram, R. H., Niwano, M., Noël, B., Ryan, J. C., Smith, A., Streffing, J., Tedesco, M., van de Berg, W. J., van den Broeke, M., van de Wal, R. S. W., van Kampenhout, L., Wilton, D., Wouters, B., Ziemen, F., and Zolles, T.: GrSMBMIP: intercomparison of the modelled 1980–2012 surface mass balance over the Greenland Ice Sheet, The Cryosphere, 14, 3935–3958, https://doi.org/10.5194/tc-14-3935-2020, 2020.

Fretwell, P., Pritchard, H. D., Vaughan, D. G., Bamber, J. L., Barrand, N. E., Bell, R., Bianchi, C., Bingham, R. G., Blankenship, D. D., Casassa, G., Catania, G., Callens, D., Conway, H., Cook, A. J., Corr, H. F. J., Damaske, D., Damm, V., Ferraccioli, F., Forsberg, R., Fujita, S., Gim, Y., Gogineni, P., Griggs, J. A., Hindmarsh, R. C. A., Holmlund, P., Holt, J. W., Jacobel, R. W., Jenkins, A., Jokat, W., Jordan, T., King, E. C., Kohler, J., Krabill, W., Riger-Kusk, M., Langley, K. A., Leitchenkov, G., Leuschen, C., Luyendyk, B. P., Matsuoka, K., Mouginot, J., Nitsche, F. O., Nogi, Y., Nost, O. A., Popov, S. V., Rignot, E., Rippin, D. M., Rivera, A., Roberts, J., Ross, N., Siegert, M. J., Smith, A. M., Steinhage, D., Studinger, M., Sun, B., Tinto, B. K., Welch, B. C., Wilson, D., Young, D. A., Xiangbin, C., and Zirizzotti, A.: Bedmap2: improved ice bed, surface and thickness datasets for Antarctica, The Cryosphere, 7, 375–393, https://doi.org/10.5194/tc-7-375-2013, 2013.

Frieler, K., Clark, P. U., He, F., Buizert, C., Reese, R., Ligtenberg, S. R., Van Den Broeke, M. R., Winkelmann, R., and Levermann, A.: Consistent evidence of increasing Antarctic accumulation with warming, Nature Climate Change, 5, 348–352, 2015.

Fürst, J. J., Durand, G., Gillet-Chaulet, F., Tavard, L., Rankl, M., Braun, M., and Gagliardini, O.: The safety band of Antarctic ice shelves,
575   Nature Climate Change, 6, 479–482, 2016.

Fyke, J., Lenaerts, J. T., and Wang, H.: Basin-scale heterogeneity in Antarctic precipitation and its impact on surface mass variability, The Cryosphere, 11, 2595–2609, 2017.

Fyke, J., Sergienko, O., Löfverström, M., Price, S., and Lenaerts, J. T.: An overview of interactions and feedbacks between ice sheets and the Earth system, Reviews of Geophysics, 56, 361–408, 2018.

580   Gallée, H.: Simulation of the Mesocyclonic Activity in the Ross Sea, Antarctica, https://doi.org/10.1175/1520-0493(1995)123<2051:SOTMAI>2.0.CO;2, 1995.

Gallée, H. and Duynkerke, P. G.: Air-snow interactions and the surface energy and mass balance over the melting zone of west Greenland during the Greenland Ice Margin Experiment, Journal of Ge, 102, 13 813–13 824, 1997.

Gallée, H. and Schayes, G.: Development of a Three-Dimensional Meso-γ Primitive Equation Model: Katabatic Winds Simulation in the
585   Area of Terra Nova Bay, Antarctica, https://doi.org/10.1175/1520-0493(1994)122<0671:DOATDM>2.0.CO;2, 1994.

Gallée, H., Guyomarc'h, G., and Brun, E.: Impact of snow drift on the antarctic ice sheet surface mass balance: Possible sensitivity to snow-surface properties, Boundary-Layer Meteorology, 99, 1–19, https://doi.org/10.1023/A:1018776422809, 2001.

Garbe, J., ALbrecht, T., Donges, J. F., and Winkelmann, R.: The hysteresis of the Antarctic Ice Sheet, Nature, 585, 538–544, 2020.

Gardner, A. S., Moholdt, G., Scambos, T., Fahnstock, M., Ligtenberg, S., Van Den Broeke, M., and Nilsson, J.: Increased West Antarctic and
590   unchanged East Antarctic ice discharge over the last 7 years, Cryosphere, 12, 521–547, 2018.

Golledge, N. R., Kowalewski, D. E., Naish, T. R., Levy, R. H., Fogwill, C. J., and Gasson, E. G.: The multi-millennial Antarctic commitment to future sea-level rise, Nature, 526, 421–425, 2015.

Gorte, T., Lenaerts, J., and Medley, B.: Scoring Antarctic surface mass balance in climate models to refine future projections, The Cryosphere Discussions, pp. 1–19, 2019.

595   Gudmundsson, G. H.: Ice-shelf buttressing and the stability of marine ice sheets, The Cryosphere, 7, 647–655, https://doi.org/https://doi.org/10.5194/tc-7-647-2013, 2013.

Hersbach, H., Bell, B., Berrisford, P., Hirahara, S., Horányi, A., Muñoz-Sabater, J., Nicolas, J., Peubey, C., Radu, R., Schepers, D., et al.: The ERA5 global reanalysis, Quarterly Journal of the Royal Meteorological Society, 2020.

Hofer, S., Tedstone, A. J., Fettweis, X., and Bamber, J. L.: Decreasing cloud cover drives the recent mass loss on the Greenland Ice Sheet,
600   Science Advances, 3, e1700 584, 2017.

Hofer, S., Lang, C., Amory, C., Kittel, C., Delhasse, A., Tedstone, A., and Fettweis, X.: Greater Greenland Ice Sheet contribution to global sea level rise in CMIP6, Nature communications, 11, 1–11, 2020.

Holland, P. R., Bracegirdle, T. J., Dutrieux, P., Jenkins, A., and Steig, E. J.: West Antarctic ice loss influenced by internal climate variability and anthropogenic forcing, Nature Geoscience, 12, 718–724, 2019.

605   Hosking, J. S., Orr, A., Bracegirdle, T. J., and Turner, J.: Future circulation changes off West Antarctica: Sensitivity of the Amundsen Sea Low to projected anthropogenic forcing, Geophysical Research Letters, 43, 367–376, 2016.

Iversen, T., Bentsen, M., Bethke, I., Debernard, J., Kirkevåg, A., Seland, Ø., Drange, H., Kristjansson, J., Medhaug, I., Sand, M., et al.: The Norwegian earth system model, NorESM1-M-part 2: Climate response and scenario projections, Geoscientific Model Development, 6, 389, 2013.

610   Kingslake, J., Ely, J. C., Das, I., and Bell, R. E.: Widespread movement of meltwater onto and across Antarctic ice shelves, Nature, 544, 349–352, 2017.

Kittel, C., Amory, C., Agosta, C., Delhasse, A., Doutreloup, S., Huot, P.-V., Wyard, C., Fichefet, T., and Fettweis, X.: Sensitivity of the current Antarctic surface mass balance to sea surface conditions using MAR, Cryosphere, 12, 3827–3839, 2018.

Krinner, G. and Flanner, M. G.: Striking stationarity of large-scale climate model bias patterns under strong climate change, Proceedings of
615   the National Academy of Sciences, 115, 9462–9466, 2018.

Krinner, G., Magand, O., Simmonds, I., Genthon, C., and Dufresne, J.-L.: Simulated Antarctic precipitation and surface mass balance at the end of the twentieth and twenty-first centuries, Climate Dynamics, 28, 215–230, 2007.

Kuipers Munneke, P., Picard, G., Van den Broeke, M., Lenaerts, J., and Van Meijgaard, E.: Insignificant change in Antarctic snowmelt volume since 1979, Geophysical Research Letters, 39, 2012.

620   Kuipers Munneke, P., Ligtenberg, S. R. M., van den Broeke, M. R., and Vaughan, D. G.: Firn air depletion as a precursor of Antarctic ice-shelf collapse, Journal of Glaciology, 60, 205–214, 2014.

Le clec'h, S., Charbit, S., Quiquet, A., Fettweis, X., Dumas, C., Kageyama, M., Wyard, C., and Ritz, C.: Assessment of the Greenland ice sheet–atmosphere feedbacks for the next century with a regional atmospheric model coupled to an ice sheet model, The Cryosphere, 13, 373–395, https://doi.org/10.5194/tc-13-373-2019, 2019.

625   Le Toumelin, L., Amory, C., Favier, V., Kittel, C., Hofer, S., Fettweis, X., Gallée, H., Kayetha, V., and Palm, S.: Accounting for drifting snow modifies atmosphere—ice-sheet interactions as simulated by MAR in Adelie Land, Antarctica, will be submitted to The Cryosphere, 14, 1713–1725, 2020(in preperation).

Lefebre, F., Gallée, H., VanYpersele, J., and Greuell, W.: Modeling of snow and ice melt at ETH Camp (West Greenland): A study of surface albedo, Journal of Geophysical Research, 108, 4231, https://doi.org/10.1029/2001JD001160, 2003.

630   Lenaerts, J. and Van den Broeke, M.: Modeling drifting snow in Antarctica with a regional climate model: 2. Results, Journal of Geophysical Research: Atmospheres, 117, 2012.

Lenaerts, J., Lhermitte, S., Drews, R., Ligtenberg, S., Berger, S., Helm, V., Smeets, C., Van Den Broeke, M., Van De Berg, W. J., Van Meijgaard, E., et al.: Meltwater produced by wind–albedo interaction stored in an East Antarctic ice shelf, Nature climate change, 7, 58–62, 2017a.

635   Lenaerts, J. T., Vizcaino, M., Fyke, J., Van Kampenhout, L., and van den Broeke, M. R.: Present-day and future Antarctic ice sheet climate and surface mass balance in the Community Earth System Model, Climate Dynamics, 47, 1367–1381, 2016.

Lenaerts, J. T., Van Tricht, K., Lhermitte, S., and L'Ecuyer, T. S.: Polar clouds and radiation in satellite observations, reanalyses, and climate models, Geophysical Research Letters, 44, 3355–3364, 2017b.

Lenaerts, J. T., Medley, B., van den Broeke, M. R., and Wouters, B.: Observing and modeling ice sheet surface mass balance, Reviews of
640   Geophysics, 57, 376–420, 2019.

Lhermitte, S., Sun, S., Shuman, C., Wouters, B., Pattyn, F., Wuite, J., Berthier, E., and Nagler, T.: Damage accelerates ice shelf instability and mass loss in Amundsen Sea Embayment, Proceedings of the National Academy of Sciences, https://doi.org/10.1073/pnas.1912890117, https://www.pnas.org/content/early/2020/09/08/1912890117, 2020.

Ligtenberg, S., Van de Berg, W., Van den Broeke, M., Rae, J., and Van Meijgaard, E.: Future surface mass balance of the Antarctic ice sheet
645   and its influence on sea level change, simulated by a regional atmospheric climate model, Climate dynamics, 41, 867–884, 2013.

Ligtenberg, S., Kuipers Munneke, P., and Van den Broeke, M.: Present and future variations in Antarctic firn air content, The Cryosphere, 8, 1711–1723, 2014.

Mauritsen, T., Bader, J., Becker, T., Behrens, J., Bittner, M., Brokopf, R., Brovkin, V., Claussen, M., Crueger, T., Esch, M., et al.: Developments in the MPI-M Earth System Model version 1.2 (MPI-ESM1. 2) and its response to increasing CO2, Journal of Advances in Modeling Earth Systems, 11, 998–1038, 2019.

Medley, B. and Thomas, E.: Increased snowfall over the Antarctic Ice Sheet mitigated twentieth-century sea-level rise, Nature Climate Change, 9, 34–39, 2019.

Medley, B., McConnell, J. R., Neumann, T., Reijmer, C., Chellman, N., Sigl, M., and Kipfstuhl, S.: Temperature and snowfall in western Queen Maud Land increasing faster than climate model projections, Geophysical Research Letters, 45, 1472–1480, 2018.

Meehl, G. A., Senior, C. A., Eyring, V., Flato, G., Lamarque, J.-F., Stouffer, R. J., Taylor, K. E., and Schlund, M.: Context for interpreting equilibrium climate sensitivity and transient climate response from the CMIP6 Earth system models, Science Advances, 6, eaba1981, 2020.

Morcrette, J.-J.: The Surface Downward Longwave Radiation in the ECMWF Forecast System, Journal of Climate, 15, 1875–1892, https://doi.org/10.1175/1520-0442(2002)015<1875:TSDLRI>2.0.CO;2, 2002.

Morlighem, M., Rignot, E., Binder, T., Blankenship, D., Drews, R., Eagles, G., Eisen, O., Ferraccioli, F., Forsberg, R., Fretwell, P., et al.: Deep glacial troughs and stabilizing ridges unveiled beneath the margins of the Antarctic ice sheet, Nature Geoscience, 13, 132–137, 2020.

Mottram, R., Hansen, N., Kittel, C., Wessem, M. v., Agosta, C., Amory, C., Boberg, F., Berg, W. J. v. d., Fettweis, X., Gossart, A., et al.: What is the Surface Mass Balance of Antarctica? An Intercomparison of Regional Climate Model Estimates, The Cryosphere Discussions, pp. 1–42, 2020.

Nowicki, S., Goelzer, H., Seroussi, H., Payne, A. J., Lipscomb, W. H., Abe-Ouchi, A., Agosta, C., Alexander, P., Asay-Davis, X. S., Barthel, A., et al.: Experimental protocol for sea level projections from ISMIP6 stand-alone ice sheet models, The Cryosphere, 14, 2331–2368, 2020.

Nowicki, S. M., Payne, T., Larour, E., Seroussi, H., Goelzer, H., Lipscomb, W., Gregory, J., Abe-Ouchi, A., and Shepherd, A.: Ice sheet model intercomparison project (ISMIP6) contribution to CMIP6, Geoscientific model development, 9, 4521, 2016.

O'Neill, B. C., Tebaldi, C., van Vuuren, D., Eyring, V., Friedlingstein, P., Hurtt, G., Knutti, R., Kriegler, E., Lamarque, J.-F., Lowe, J., et al.: The Scenario Model Intercomparison Project (ScenarioMIP) for CMIP6, Geoscientific Model Development, 9, 3461–3482, 2016.

Palerme, C., Genthon, C., Claud, C., Kay, J. E., Wood, N. B., and L'Ecuyer, T.: Evaluation of current and projected Antarctic precipitation in CMIP5 models, Climate dynamics, 48, 225–239, 2017.

Paolo, F. S., Fricker, H. A., and Padman, L.: Volume loss from Antarctic ice shelves is accelerating, Science, 348, 327–331, 2015.

Pattyn, F., Ritz, C., Hanna, E., Asay-Davis, X., DeConto, R., Durand, G., Favier, L., Fettweis, X., Goelzer, H., Golledge, N. R., et al.: The Greenland and Antarctic ice sheets under 1.5 C global warming, Nature Climate Change, 8, 1053–1061, 2018.

Previdi, M. and Polvani, L. M.: Anthropogenic impact on Antarctic surface mass balance, currently masked by natural variability, to emerge by mid-century, Environmental Research Letters, 11, 094 001, 2016.

Raphael, M. N., Marshall, G., Turner, J., Fogt, R., Schneider, D., Dixon, D., Hosking, J., Jones, J., and Hobbs, W. R.: The Amundsen sea low: variability, change, and impact on Antarctic climate, Bulletin of the American Meteorological Society, 97, 111–121, 2016.

Rignot, E., Casassa, G., Gogineni, P., Krabill, W., Rivera, A., and Thomas, R.: Accelerated ice discharge from the Antarctic Peninsula following the collapse of Larsen B ice shelf, Geophysical research letters, 31, 2004.

Rignot, E., Mouginot, J., Scheuchl, B., van den Broeke, M., van Wessem, M. J., and Morlighem, M.: Four decades of Antarctic Ice Sheet mass balance from 1979–2017, Proceedings of the National Academy of Sciences, 116, 1095–1103, 2019.

685   Ritz, C., Edwards, T. L., Durand, G., Payne, A. J., Peyaud, V., and Hindmarsh, R. C.: Potential sea-level rise from Antarctic ice-sheet instability constrained by observations, Nature, 528, 115–118, 2015.

Scambos, T. A., Hulbe, C., Fahnestock, M., and Bohlander, J.: The link between climate warming and break-up of ice shelves in the Antarctic Peninsula, Journal of Glaciology, 46, 516–530, 2000.

Scambos, T. A., Bohlander, J., Shuman, C. A., and Skvarca, P.: Glacier acceleration and thinning after ice shelf collapse in the Larsen B
690   embayment, Antarctica, Geophysical Research Letters, 31, 2004.

Scambos, T. A., Berthier, E., Haran, T., Shuman, C. A., Cook, A. J., Ligtenberg, S. R. M., and Bohlander, J.: Detailed ice loss pattern in the northern Antarctic Peninsula: widespread decline driven by ice front retreats, The Cryosphere, 8, 2135–2145, https://doi.org/10.5194/tc-8-2135-2014, 2014.

Sellar, A. A., Jones, C. G., Mulcahy, J. P., Tang, Y., Yool, A., Wiltshire, A., O'Connor, F. M., Stringer, M., Hill, R., Palmieri, J., Woodward,
695   S., de Mora, L., Kuhlbrodt, T., Rumbold, S. T., Kelley, D. I., Ellis, R., Johnson, C. E., Walton, J., Abraham, N. L., Andrews, M. B., Andrews, T., Archibald, A. T., Berthou, S., Burke, E., Blockley, E., Carslaw, K., Dalvi, M., Edwards, J., Folberth, G. A., Gedney, N., Griffiths, P. T., Harper, A. B., Hendry, M. A., Hewitt, A. J., Johnson, B., Jones, A., Jones, C. D., Keeble, J., Liddicoat, S., Morgenstern, O., Parker, R. J., Predoi, V., Robertson, E., Siahaan, A., Smith, R. S., Swaminathan, R., Woodhouse, M. T., Zeng, G., and Zerroukat, M.: UKESM1: Description and Evaluation of the U.K. Earth System Model, Journal of Advances in Modeling Earth Systems, 11, 4513–4558,
700   https://doi.org/10.1029/2019MS001739, 2019.

Seroussi, H., Nowicki, S., Payne, A. J., Goelzer, H., Lipscomb, W. H., Abe Ouchi, A., Agosta, C., Albrecht, T., Asay-Davis, X., Barthel, A., et al.: ISMIP6 Antarctica: a multi-model ensemble of the Antarctic ice sheet evolution over the 21st century, The Cryosphere Discussions, 2020.

Shepherd, A., Ivins, E., Rignot, E., Smith, B., van den Broeke, M., Velicogna, I., Whitehouse, P., Briggs, K., Joughin, I., Krinner, G.,
705   Nowicki, S., Payne, T., Scambos, T., Schlegel, N., A, G., Agosta, C., Ahlström, A., Babonis, G., Barletta, V., Blazquez, A., Bonin, J., Csatho, B., Cullather, R., Felikson, D., Fettweis, X., Forsberg, R., Gallee, H., Gardner, A., Gilbert, L., Groh, A., Gunter, B., Hanna, E., Harig, C., Helm, V., Horvath, A., Horwath, M., Khan, S., Kjeldsen, K. K., Konrad, H., Langen, P., Lecavalier, B., Loomis, B., Luthcke, S., McMillan, M., Melini, D., Mernild, S., Mohajerani, Y., Moore, P., Mouginot, J., Moyano, G., Muir, A., Nagler, T., Nield, G., Nilsson, J., Noel, B., Otosaka, I., Pattle, M. E., Peltier, W. R., Pie, N., Rietbroek, R., Rott, H., Sandberg-Sørensen, L., Sasgen, I., Save, H., Scheuchl,
710   B., Schrama, E., Schröder, L., Seo, K.-W., Simonsen, S., Slater, T., Spada, G., Sutterley, T., Talpe, M., Tarasov, L., van de Berg, W. J., van der Wal, W., van Wessem, M., Vishwakarma, B. D., Wiese, D., Wouters, B., and team, T. I.: Mass balance of the Antarctic Ice Sheet from 1992 to 2017, Nature, 558, 219–222, https://doi.org/10.1038/s41586-018-0179-y, 2018.

Taylor, K. E., Stouffer, R. J., and Meehl, G. A.: An overview of CMIP5 and the experiment design, Bulletin of the American Meteorological Society, 93, 485–498, 2012.

715   Tedesco, M., Doherty, S., Fettweis, X., Alexander, P., Jeyaratnam, J., and Stroeve, J.: The darkening of the Greenland ice sheet: trends, drivers, and projections (1981–2100), The Cryosphere, 10, 477–496, 2016.

Trusel, L. D., Frey, K. E., Das, S. B., Karnauskas, K. B., Munneke, P. K., Van Meijgaard, E., and Van Den Broeke, M. R.: Divergent trajectories of Antarctic surface melt under two twenty-first-century climate scenarios, Nature Geoscience, 8, 927–932, 2015.

van den Broeke, M.: Strong surface melting preceded collapse of Antarctic Peninsula ice shelf, Geophysical Research Letters, 32, 2005.

720   Van Wessem, J. M., Jan Van De Berg, W., Noël, B. P., Van Meijgaard, E., Amory, C., Birnbaum, G., Jakobs, C. L., Krüger, K., Lenaerts, J., Lhermitte, S., et al.: Modelling the climate and surface mass balance of polar ice sheets using racmo2: Part 2: Antarctica (1979-2016), Cryosphere, 12, 1479–1498, 2018.

Vieli, A., Payne, A. J., Shepherd, A., and Du, Z.: Causes of pre-collapse changes of the Larsen B ice shelf: Numerical modelling and assimilation of satellite observations, Earth and Planetary Science Letters, 259, 297–306, 2007.

725 Voldoire, A., Saint-Martin, D., Sénési, S., Decharme, B., Alias, A., Chevallier, M., Colin, J., Guérémy, J.-F., Michou, M., Moine, M.-P., et al.: Evaluation of CMIP6 deck experiments with CNRM-CM6-1, Journal of Advances in Modeling Earth Systems, 11, 2177–2213, 2019.

Wille, J. D., Favier, V., Dufour, A., Gorodetskaya, I. V., Turner, J., Agosta, C., and Codron, F.: West Antarctic surface melt triggered by atmospheric rivers, Nature Geoscience, 12, 911–916, 2019.

Wyser, K., Noije, T. v., Yang, S., Hardenberg, J. v., O'Donnell, D., and Döscher, R.: On the increased climate sensitivity in the EC-Earth
730 model from CMIP5 to CMIP6, Geoscientific Model Development, 13, 3465–3474, 2020.

Zelinka, M. D., Myers, T. A., McCoy, D. T., Po-Chedley, S., Caldwell, P. M., Ceppi, P., Klein, S. A., and Taylor, K. E.: Causes of higher climate sensitivity in CMIP6 models, Geophysical Research Letters, 47, e2019GL085 782, 2020.

Zhu, J., Poulsen, C. J., and Otto-Bliesner, B. L.: High climate sensitivity in CMIP6 model not supported by paleoclimate, Nature Climate Change, 10, 378–379, 2020.